Steel and Composite Structures, *Vol. 31, No. 0 (2019) 000-000*
DOI: https://doi.org/10.12989/scs.2019.31.0.000

Nonlinear buckling and post-buckling of functionally graded CNTs reinforced composite truncated conical shells subjected to axial load

Do Quang Chan [1a], Pham Dinh Nguyen [2a], Vu Dinh Quang [2b], Vu Thi Thuy Anh [2c] and Nguyen Dinh Duc [*2,3,4]

[1] *University of Transport Technology, Hanoi - 54 Trieu Khuc, Thanh Xuan, Hanoi, Vietnam*
[2] *Avanced Materials and Structures Laboratory, University of Engineering and Technology, 144 Xuan Thuy, Cau Giay, Hanoi, Viet Nam*
[3] *Vietnam-Japan University, Luu Huu Phuoc, My Dinh 1, Nam Tu Liem, Ha Noi, Viet Nam*
[4] *National Research Laboratory, Department of Civil and Environmental Engineering, Sejong University, 209 Neungdong-ro, Gwangjin-gu, Seoul 05006, Korea*

(*Received May 8, 2018, Revised March 29, 2019, Accepted April 4, 2019*)

Abstract. This study deals with the nonlinear static analysis of functionally graded carbon nanotubes reinforced composite (FG-CNTRC) truncated conical shells subjected to axial load based on the classical shell theory. Detailed studies for both nonlinear buckling and post-buckling behavior of truncated conical shells. The truncated conical shells are reinforced by single-walled carbon nanotubes which alter according to linear functions of the shell thickness. The nonlinear equations are solved by both the Airy stress function and Galerkin method based on the classical shell theory. In numerical results, the influences of various types of distribution and volume fractions of carbon nanotubes, geometrical parameters, elastic foundations on the nonlinear buckling and post-buckling behavior of FG-CNTRC truncated conical shells are presented. The proposed results are validated by comparing with other authors.

Keywords: nonlinear buckling and post-buckling; FG-CNTRC; truncated conical shells; galerkin method

1. Introduction

The truncated conical shells are important components as principal elements of engineering structures which draw attention to researchers and scientists. As well as known, there are many authors study the static and dynamic analysis of truncated conical shells made of different materials. One of the most renowned authors on these structures is Sofiyev with some investigations by him and his co-workers were reported in the literature (Sofiyev and Schnack 2003, Sofiyev 2010, 2011, 2015, Najafov and Sofiyev 2013, Sofiyev and Kuruoglu 2013, 2015, 2016, Sofiyev *et al*. 2017). It can be seen that, in Sofiyev's studies, he analyzed, in turn, the linear and nonlinear buckling behavior, dynamic and the free vibration analysis of truncated conical shells surrounded or not by an elastic medium under different loads. He used the form of one-component deflection function for linear studies and the form of two-component deflection function for nonlinear studies to solve the system of nonlinear partial differential equations. His studies were obtained for truncated conical shells by using the stress function, the deflection function and the superposition method.

*Corresponding author, Ph.D., Professor,
E-mail: ducnd@vnu.edu.vn
[a] Ph.D. Student
[b] Master's Student
[c] Ph.D.

These novel researches about buckling analysis of conical and truncated conical shells made of composite materials are studied. Buckling analyses of laminated truncated conical shells subjected to external hydrostatic compression are carried out by Hu and Chen (2018). Shadmehri *et al*. (2012) investigated the linear buckling response of conical composite shells under compression load using the first-order shear deformation shell theory. Seidi *et al*. (2015) presented the temperature-dependent buckling analysis of sandwich conical shell with thin functionally graded facesheets and homogenous soft core based on analytical solution. Morozov *et al*. (2011) investigated the buckling analysis and design of anisogrid composite lattice conical shells. Zielnica (2012) studied the buckling and stability of elastic-plastic sandwich conical shells. Sharghi *et al*. (2016) studied the buckling of generally laminated conical shells with various boundary conditions subjected to axial pressure is studied using an analytical approach. Topal (2013) investigated the pareto optimum design of laminated composite truncated circular conical shells.

In addition, there are many works have focused on buckling and post-buckling behaviors of functionally graded materials (FGM) truncated conical shells. Thermal buckling analysis of FGM sandwich truncated conical shells reinforced by FGM stiffeners resting on elastic foundations using FSDT are carried out by Duc *et al*. (2018). Khayat *et al*. (2017) investigated the buckling analysis of functionally graded truncated conical shells under external displacement-dependent pressure. The an analytical investigation for

ISSN: 1229-9367 (Print), 1598-6233 (Online)

analyzing the buckling and post-buckling behaviors of truncated conical shells made of FGM subjected to axial compressive load and external uniform pressure are presented by Dung *et al*. (2017) and Chan *et al*. (2018). Torabi *et al*. (2013) studied the buckling analysis of a FGM conical shell integrated with piezoelectric layers subjected to combined action of thermal and electrical loads. Naj *et al*. (2008) investigated the thermal and mechanical instability of functionally graded truncated conical shells. Akbari *et al*. (2015) presented the thermal buckling of temperature-dependent FGM conical shells with arbitrary edge supports based on an iterative generalized differential quadrature method. Duc and Cong (2015) studied the thermal stability of an eccentrically stiffened functionally graded truncated conical shells in thermal environment and surrounded on elastic foundations. Viola *et al*. (2014) investigated the static analysis of FGM conical shells and panels using the generalized unconstrained third order theory coupled with the stress recovery.

FG-CNTRC were first proposed by Shen (2009) and until now, FG-CNTRC have become more popular and recently, researchers have paid much heed to the development of FG-CNTRC. In particular, up to this point, studies on the linear and nonlinear of FG-CNTRC conical and truncated conical shells are also of more interest to researchers. The typical studies for static and dynamic analysis of FG-CNTRC truncated conical shells include, via the extended Hamilton principle, Heydarpour *et al*. (2014) discretized the governing differential equations subjected to the related boundary conditions for studying free vibration analysis of rotating FG-CNTRC truncated conical shells by using the differential quadrature method. Duc and Nguyen (2017) studied the dynamic response and vibration of FG-CNTRC truncated conical shells resting on elastic foundation based on the classical shell theory. Kamarian *et al*. (2016) investigated the free vibration analysis of CNTRC conical shells based on first-order shear deformation theory. Mehri *et al*. (2016a, b) studied the on dynamic instability of a FG-CNTRC truncated conical shell under simultaneous actions of a hydrostatic pressure and yawed supersonic airflow and the buckling and vibration of the FG-CNTRC truncated conical shell subjected to axial compression and external pressure simultaneously based on the basis of Novozhilov nonlinear shell theory and Green-Lagrange geometrical nonlinearity and using Fourier expansion and the harmonic differential quadrature. Ansari and Torabi (2016) studied the buckling and vibration of FG-CNTRC conical shells under axial loading by using the generalized differential quadrature method. By using first order theory of shells and geometrical non-linearity of von-Karman and Donnell kinematic assumptions and according to the adjacent equilibrium criterion, Jam and Kiani (2016) dealt with the buckling of FG-CNTRC conical shells subjected to pressure loading. Mirzaei and Kiani (2015) presented the thermal buckling of FG-CNTRC conical shells with axially immovable edge supports subjected to uniform temperature rise loading. With the equilibrium and linearized stability equations for the shells are derived based on the classical shell theory, Duc *et al*. (2017) studied the linear thermal and mechanical instability of the FG-CNTRC truncated conical shells in thermal environment.

Despite all the above-mentioned literature, it is clear that the buckling and post-buckling behaviors are very important for understanding the structural responses of truncated conical shells as well as scientific foundations for structural designers, manufacturers and for building projects using this structure, however, the number of works for FG-CNTRC truncated conical shells is still limited. The majority of publications is focused on linear buckling and free vibration analysis of truncated conical shells. Thus, this work proposes to analyze the nonlinear buckling and post-buckling behaviors of FG-CNTRC truncated conical shells subjected to axial load using the classical shell theory.

2. Material properties and formulation

2.1 Numerical simulation procedure

The FG-CNTRC material is made of Poly (methyl methacrylate), referred to as PMMA, reinforced by (10,10) single-walled carbon nanotubes (SWCNTs). The SWCNT reinforcement is functionally graded (FG) or uniformly distributed (UD) in the thickness direction (Shen 2009, Duc and Nguyen 2017). Four types of FG-CNTRCs, i.e., FG-Λ, FG-X, FG-O and UD CNTRC (Fig. 1), which are the functionally graded distraction of CNTs through the thickness direction of the composite truncated conical shell, will be investigated in this work.

The volume fractions of component materials are assumed to vary according to the linear functions of the shell thickness are expressed as follows (Shen 2009, Heydarpour *et al*. 2014, Duc and Nguyen 2017)

$$V_{CNT}=\begin{cases} V_{CNT}^{*} & (\text{UD}) \\ V_{CNT}^{*}\left(1-2\dfrac{z}{h}\right) & (\text{FG-}\Lambda) \\ 2V_{CNT}^{*}\left(1-2\dfrac{|z|}{h}\right) & (\text{FG-O}) \\ 4V_{CNT}^{*}\dfrac{|z|}{h} & (\text{FG-X}) \end{cases}, V_{m}=1-V_{CNT}. \tag{1}$$

where

$$V_{CNT}^{*}=\frac{w_{CNT}}{w_{CNT}+\left(\rho_{CNT}/\rho_{m}\right)-\left(\rho_{CNT}/\rho_{m}\right)w_{CNT}}, \tag{2}$$

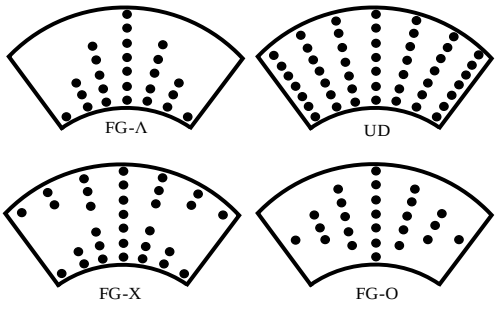

Fig. 1 Configurations of CNTRC truncated conical shells

in which w_{CNT} is the mass fraction of CNTs, and ρ_{CNT} and ρ_m are the densities of CNT and matrix, respectively.

The effective Poisson's ratio may be written as (Shen 2009)

$$v_{12} = V_{CNT}^{*} v_{12}^{CNT} + V_m v^m \tag{3}$$

where v_{12}^{CNT} and v_m are Poisson's ratio of the CNT and the matrix, respectively.

There E_{11}^{CNT}, E_{11}^{CNT}, G_{12}^{CNT} are Young's and shear modulus of the CNT, respectively; E_m, G_m are mechanical properties of the matrix, η_i $(i = \overline{1,3})$ are the CNT efficiency parameters and V_{CNT} and V_m are the volume fractions of the CNT and the matrix, respectively, the elastic modules of the FG-CNTRC material are determined as (Shen 2009)

$$\begin{aligned} E_{11} &= \eta_1 V_{CNT} E_{11}^{CNT} + V_m E_m, \\ \frac{\eta_2}{E_{22}} &= \frac{V_{CNT}}{E_{22}^{CNT}} + \frac{V_m}{E_m}, \\ \frac{\eta_3}{G_{12}} &= \frac{V_{CNT}}{G_{12}^{CNT}} + \frac{V_m}{G_m}, \end{aligned} \tag{4}$$

The CNT efficiency parameters η_i $(i = \overline{1,3})$ used in Eq. (4) are estimated by matching Young's modulus E_{11} and E_{22} and the shear modulus G_{12} of FG-CNTRC material obtained by the extended rule of mixture to molecular simulation results (Shen 2009). For three different volume fraction of CNTs, these parameters are as: η_1 = 0.137, η_2 = 1.022, η_3 = 0.715 for the case of V_{CNT}^{*} 0.12; η_1 = 0.142, η_2 = 1.626, η_3 = 1.138 for the case of V_{CNT}^{*} 0.17 and η_1 = 0.141, η_2 = 1.585, η_3 = 1.109 for the case of V_{CNT}^{*} = 0.28. (Heydarpour *et al*. 2014, Duc and Nguyen 2017).

2.2 Model FG-CNTRC truncated conical shells resting on elastic foundations

Consider a thin FG-CNTRC truncated conical shells surrounded by the elastic foundations, with the shell of thickness h, radii $R_1 < R_2$, length L and the semi-vertex angle of the cone γ. The meridional, circumferential, and normal directions of the shell are denoted by S, θ and z, respectively. A schematic of the shell with the assigned coordinate system and geometric characteristics are shown in Fig. 2.

The FG-CNTRC truncated conical shell is surrounded by an elastic medium. The reaction-deflection relation of foundation is given by (Sofiyev 2011)

$$q_e(S,\varphi) = K_w w - K_p \Delta w, \tag{5}$$

where $\varphi = \theta \sin(\gamma)$; $\Delta w = \left(\frac{\partial^2 w}{\partial S^2} + \frac{1}{S}\frac{\partial w}{\partial S} + \frac{1}{S^2}\frac{\partial^2 w}{\partial \varphi^2}\right)$; w is the deflection of the shell, K_w (N/m^3) is the spring layer foundation stiffness and K_p (N/m) is the shear layer foundation stiffness of Pasternak foundation.

2.3 Theoretical formulations

In this study, the basic equations of thin FG-CNTRC truncated conical shells are achieved by using the classical shell theory. The strains across the shell thickness at a distance z from the mid-plane are

$$\begin{Bmatrix} \varepsilon_S \\ \varepsilon_\theta \\ \gamma_{S\theta} \end{Bmatrix} = \begin{Bmatrix} \varepsilon_S^0 \\ \varepsilon_\theta^0 \\ \gamma_{S\theta}^0 \end{Bmatrix} + z \begin{Bmatrix} k_S \\ k_\theta \\ 2k_{S\theta} \end{Bmatrix}. \tag{6}$$

Taking into account Von Karman – Donnell nonlinear terms, the strains at the middle surface and the change of curvatures and twist are related to the displacement components u, v, w in the S, θ, z. coordinate directions, respectively, as (Sofiyev 2011)

$$\begin{aligned} &\varepsilon_S^0 = \frac{\partial u}{\partial S} + \frac{1}{2}\left(\frac{\partial w}{\partial S}\right)^2, \varepsilon_\theta^0 = \frac{1}{S}\frac{\partial v}{\partial \varphi} + \frac{u}{S} - \frac{w}{S}\cot\gamma + \frac{1}{2S^2}\left(\frac{\partial w}{\partial \varphi}\right)^2 \\ &\gamma_{S\theta}^0 = 2\left[\frac{1}{S}\frac{\partial u}{\partial \varphi} - \frac{v}{S} + \frac{\partial v}{\partial S} + \frac{1}{S}\left(\frac{\partial w}{\partial S}\frac{\partial w}{\partial \varphi}\right)^2\right], \\ &k_S = -\frac{\partial^2 w}{\partial S^2}, k_\theta = -\frac{1}{S^2}\frac{\partial^2 w}{\partial \varphi^2} - \frac{1}{S}\frac{\partial w}{\partial S}, \\ &k_{S\theta} = -\frac{1}{S}\frac{\partial^2 w}{\partial S \partial \varphi} + \frac{1}{S^2}\frac{\partial w}{\partial \varphi}. \end{aligned} \tag{7}$$

with ε_S^0 and ε_θ^0 are the normal strains in the curvilinear coordinate directions S and θ on the reference surface respectively, $\gamma_{S\theta}^0$ is the shear strain at the middle surface of the shell, k_S, k_θ, $k_{S\theta}$ are the changes of curvatures and twist.

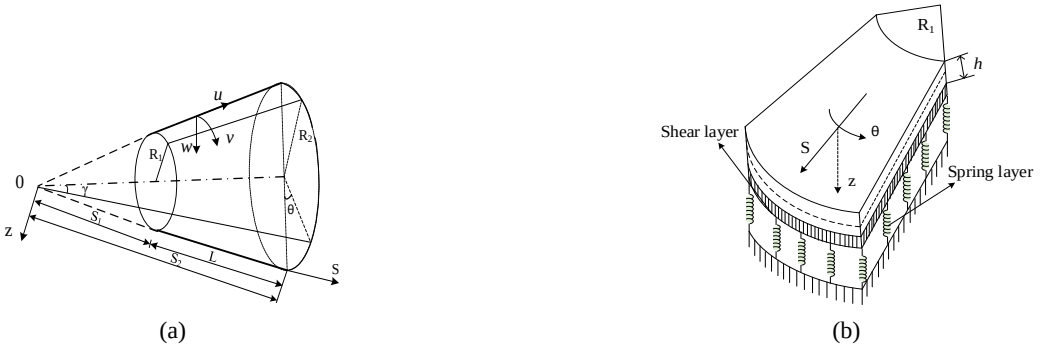

(a) (b)

Fig. 2 The geometry of a FG-CNTRC truncated conical shell resting on elastic foundations

Using Eqs. (6) and (7), the nonlinear geometrical compatibility equation of truncated conical shells is written as

$$\begin{aligned}&\frac{\cot\gamma}{S}\frac{\partial^2 w}{\partial S^2}-\frac{1}{S}\frac{\partial^2\gamma_{S\theta}^0}{\partial S\partial\varphi}-\frac{1}{S^2}\frac{\partial\gamma_{S\theta}^0}{\partial\varphi}+\frac{\partial^2\varepsilon_\theta^0}{\partial S^2}+\frac{1}{S^2}\frac{\partial^2\varepsilon_S^0}{\partial\varphi^2}\\&+\frac{2}{S}\frac{\partial\varepsilon_\theta^0}{\partial S}-\frac{1}{S}\frac{\partial\varepsilon_S^0}{\partial S}=\frac{1}{S^4}\left(\frac{\partial w}{\partial\varphi}\right)^2-\frac{2}{S^3}\frac{\partial w}{\partial\varphi}\frac{\partial^2 w}{\partial S\partial\varphi}\\&-\frac{1}{S^2}\left[\frac{\partial^2 w}{\partial S^2}\frac{\partial^2 w}{\partial\varphi^2}-\left(\frac{\partial^2 w}{\partial S\partial\varphi}\right)^2\right]-\frac{1}{S}\frac{\partial w}{\partial S}\frac{\partial^2 w}{\partial S^2}.\end{aligned}\tag{8}$$

The stress-strain relations of the shell are given as

$$\begin{bmatrix}\sigma_S\\ \sigma_\theta\\ \sigma_{S\theta}\end{bmatrix}=\begin{bmatrix}Q_{11}&Q_{12}&0\\ Q_{12}&Q_{22}&0\\ 0&0&Q_{66}\end{bmatrix}\begin{bmatrix}\varepsilon_S\\ \varepsilon_\theta\\ \gamma_{S\theta}\end{bmatrix},\tag{9}$$

in which, the quantities Q_{ij}, (ij = 11, 12, 22, 66) are functions of non-dimensional thickness coordinate

$$Q_{11}=\frac{E_{11}}{1-\nu_{12}\nu_{21}},\ Q_{22}=\frac{E_{22}}{1-\nu_{12}\nu_{21}},$$
$$Q_{12}=\frac{\nu_{21}E_{11}}{1-\nu_{12}\nu_{21}},\ Q_{66}=G_{12},$$

The force and moment resultants of FG-CNTRC shells are shown by

$$\left(N_i,M_i\right)=\int_{-h/2}^{h/2}\sigma_i(1,z)\,dz,\ \left(i=s,\theta\right).\tag{10}$$

The force and moment resultants of the shell are expressed in terms of the stress components through the thickness

$$\begin{Bmatrix}N_S\\ N_\theta\\ N_{S\theta}\\ M_S\\ M_\theta\\ M_{S\theta}\end{Bmatrix}=\begin{bmatrix}A_{11}&A_{12}&0&B_{11}&B_{12}&0\\ A_{12}&A_{22}&0&B_{12}&B_{22}&0\\ 0&0&A_{66}&0&0&2B_{66}\\ B_{11}&B_{12}&0&D_{11}&D_{12}&0\\ B_{12}&B_{22}&0&D_{12}&D_{22}&0\\ 0&0&B_{66}&0&0&2D_{66}\end{bmatrix}\begin{Bmatrix}\varepsilon_S^0\\ \varepsilon_\theta^0\\ \gamma_{S\theta}^0\\ k_s\\ k_\theta\\ k_{S\theta}\end{Bmatrix},\tag{11}$$

where the coefficients A_{ij}, B_{ij}, D_{ij} (i, j = 1 – 2, 6) are shown by

$$\left(A_{ij},B_{ij},D_{ij}\right)=\int_{-h/2}^{h/2}Q_{ij}(1,z,z^2)\,dz.\tag{12}$$

The nonlinear equilibrium equations of a truncated conical shell (Sofiyev 2011)

$$\begin{aligned}&S\frac{\partial N_S}{\partial S}+\frac{\partial N_{S\theta}}{\partial\varphi}+N_S-N_\theta=0,\\&\frac{\partial N_\theta}{\partial\varphi}+S\frac{\partial N_{S\theta}}{\partial S}+2N_{S\theta}=0,\end{aligned}\tag{13}$$

$$\begin{aligned}&S\frac{\partial^2 M_S}{\partial S^2}+2\frac{\partial M_S}{\partial S}+2\left(\frac{\partial^2 M_{S\theta}}{\partial S\partial\varphi}+\frac{1}{S}\frac{\partial M_{S\theta}}{\partial\varphi}\right)+\frac{1}{S}\frac{\partial^2 M_\theta}{\partial\varphi^2}\\&-\frac{\partial M_\theta}{\partial S}-N_\theta\cot\gamma+\frac{\partial}{\partial S}\left(SN_S\frac{\partial w}{\partial S}+N_{S\theta}\frac{\partial w}{\partial\varphi}\right)\\&+\frac{\partial}{\partial\varphi}\left(N_{S\theta}\frac{\partial w}{\partial S}+\frac{1}{S}N_\theta\frac{\partial w}{\partial\varphi}\right)-SK_w w+SK_p\Delta w=0.\end{aligned}\tag{13}$$

The first two equations of the system of Eq. (13) are satisfied by using a stress function F as (Sofiyev 2011)

$$\begin{aligned}&N_S=\frac{1}{S^2}\frac{\partial^2 F}{\partial\varphi^2}+\frac{1}{S}\frac{\partial F}{\partial S},\qquad N_\theta=\frac{\partial^2 F}{\partial S^2},\\&N_{S\theta}=-\frac{1}{S}\frac{\partial^2 F}{\partial S\partial\varphi}+\frac{1}{S^2}\frac{\partial F}{\partial\varphi}.\end{aligned}\tag{14}$$

Substituting Eqs. (6), (11), (14) into the Eq. (8) and Eqs. (6), (11), (14) into the third equation of the system (13), obtained two new equations of F and w. For the simplicity of the mathematical operations, the variable $S = S_1e^x$ is included and $F = F_1e^{2x}$ is taken into account instead of F, after lengthy computations, the system of nonlinear partial differential equations for F_1 and w can be shown in the form as

$$\begin{aligned}&H_{11}\left(F_1\right)+H_{12}\left(w\right)+H_{13}\left(F_1,w\right)=0,\\&H_{21}\left(F_1\right)+H_{22}\left(w\right)+H_{23}\left(w,w\right)=0.\end{aligned}\tag{15}$$

with H_{ij} are given in Appendix I.

The system Eqs. (15) are basic equations to analyze both the nonlinear buckling and post-buckling behavior of FG-CNTRC truncated conical shells resting on elastic foundations.

2.4 Boundary condition and solution

In this section, the main equation of FG-CNTRC truncated conical shells are achieved. The truncated conical shell is assumed to be simply supported at both edges

$$w=0\quad\text{at}\quad x=0\quad\text{and}\quad x=x_0.\tag{16}$$

The boundary condition can be satisfied when the deflection w is approximately assumed as follows (Sofiyev 2011)

$$w=fe^x\sin(m_1x)\sin(m_2\theta)+Gfe^x\sin^2\left(m_1x\right),\tag{17}$$

where $m_1=\frac{m\pi}{x_0}$, $m_2=\frac{n}{\sin\gamma}$, $x_0=\ln\frac{S_2}{S_1}$, m is the numbers of half waves along a generatrix and n is number of full waves along a parallel circle. There is form of two-component deflection function, f is the unknown amplitude of the deflection in the linear case and G is a parameter that determines relationship between the linear and nonlinear parts of the displacement of deflection function or in other words, with respect to the space configuration, the first term corresponds to that used in the stability theory of infinitesimal deflections and the second term reflects the preferred inward bulging of the conical shell when the displacements become large.

Substituting Eqs. (17) into Eqs. (15) and solving the obtained equation by applying the superposition principle, the stress function F_1 can be obtained as

$$\begin{aligned}
F_1 &= K_1 f e^{-x}\sin(m_1 x)\sin(m_2\varphi)+K_2 f e^{-x}\cos(m_1 x)\sin(m_2\varphi)\\
&+K_3 G f\, e^{-x}\cos(2m_1 x)+K_4 G f\, e^{-x}\sin(2m_1 x)\\
&+\left(K_{51}G^2 f+K_{52}+K_{53}G\right) f\cos(2m_1 x)\\
&+\left(K_{61}G^2 f+K_{62}+K_{63}G\right) f\sin(2m_1 x)\\
&+K_7 f^2\cos(2m_1 x)\cos(2m_2\varphi)+K_8 f^2\sin(2m_1 x)\cos(2m_2\varphi)\\
&+\left(K_{91}Gf^2+K_{92}f\right)\cos(m_1 x)\sin(m_2\varphi)\\
&+\left(K_{101}Gf^2+K_{102}f\right)\sin(m_1 x)\sin(m_2\varphi)+\\
&+K_{11}Gf^2\cos(3m_1 x)\sin(m_2\varphi)+K_{12}Gf^2\sin(3m_1 x)\sin(m_2\varphi)\\
&+K_{13}G^2 f^2\cos(4m_1 x)+K_{14}G^2 f^2\sin(4m_1 x)\\
&+K_{15}f^2\cos(2m_2\varphi)+K_{16}Gfe^{-x}-\frac{1}{2}\left(1+e^{2x}\cos(m_2\varphi)\right)TS_1^2.
\end{aligned} \tag{18}$$

where the following definitions apply

$$K_1=-\frac{a_{24}}{a_{23}},K_2=-\frac{a_{25}}{a_{23}},K_3=\frac{a_{13}}{a_{12}},K_4=\frac{a_{14}}{a_{12}},K_{51}=-\frac{1}{2}\frac{m_1\left(2a_{15}m_1+a_{16}\right)}{a_{15}^2+a_{16}^2},$$

$$K_{52}=-\frac{a_{15}a_{17}+a_{16}a_{18}}{a_{15}^2+a_{16}^2},K_{53}=-\frac{\cot(\gamma)S_1m_1\left(2a_{15}m_1+a_{16}\right)}{a_{15}^2+a_{16}^2},$$

$$K_{61}=-\frac{1}{2}\frac{m_1\left(-2a_{16}m_1+a_{15}\right)}{a_{15}^2+a_{16}^2},K_{62}=-\frac{a_{15}a_{18}-a_{16}a_{17}}{a_{15}^2+a_{16}^2},$$

$$K_{63}=-\frac{\cot(\gamma)S_1m_1\left(-2a_{16}m_1+a_{15}\right)}{a_{15}^2+a_{16}^2},K_7=\frac{1}{4}\frac{a_1m_1^2-4a_2a_3}{a_1^2+a_2^2},$$

$$K_8=\frac{1}{2}\frac{a_2m_1^2+4a_1a_3}{a_1^2+a_2^2},K_{91}=-\frac{a_{19}a_{21}+a_{20}a_{22}}{a_{19}^2+a_{20}^2},$$

$$K_{92}=\frac{1}{2}\frac{\cot(\gamma)S_1m_1\left(a_{19}m_1-a_{20}\right)}{a_{19}^2+a_{20}^2},K_{101}=\frac{a_{19}a_{22}-a_{20}a_{21}}{a_{19}^2+a_{20}^2},$$

$$K_{102}=\frac{1}{2}\frac{\cot(\gamma)S_1m_1\left(a_{20}m_1+a_{19}\right)}{a_{19}^2+a_{20}^2},K_{11}=-\frac{a_8a_{10}-a_9a_{11}}{a_8^2+a_9^2},$$

$$K_{12}=-\frac{a_8a_{11}+a_9a_{10}}{a_8^2+a_9^2},K_{13}=\frac{a_4m_1^2+a_5a_6}{a_4^2+a_5^2},$$

$$K_{14}=\frac{a_5m_1^2-a_4a_6}{a_4^2+a_5^2},K_{15}=\frac{m_1^2m_2^2}{2a_7},K_{16}=-\frac{c_{12}+c_{21}}{2A_{22}^*}.$$

in which the remaining constants a_i ($i = 1 \div 25$) are given in Appendix II.

Applying the Galerkin method with the limits of integral is given by the formula

$$\int_0^{x_0}\int_0^{2\pi\sin\gamma}\Phi e^x\sin(m_1x)\sin(m_2\varphi)d\varphi dx=0, \tag{19}$$

$$\int_0^{x_0}\int_0^{2\pi\sin\gamma}\Phi e^x\sin^2(m_1x)d\varphi dx=0, \tag{20}$$

where Φ is the left hand side of the first equation of system Eq. (15) after substitution Eqs. (19)-(20), after that, we obtain the following equations

$$u_1f^2G^2+u_2fG+u_3f^2+u_4T+u_5=0, \tag{21}$$

$$u_6G^3f^3+u_7f^2G^2+u_8f^3G+u_{10}fG+u_{11}f^2+\left(u_9fG+u_{12}\right)T=0. \tag{22}$$

where the constants u_i, i = (1 – 12) are given in Appendix III.

From Eqs. (21) and (22) lead to the relationship between the linear and nonlinear parts of the displacement as follows

$$\begin{aligned}
&-\frac{\left(u_1u_9-u_4u_6\right)f^3G^3}{u_4}-\frac{\left(u_1u_{12}+u_2u_9-u_4u_7\right)f^2G^2}{u_4}\\
&+\left(-\frac{\left(u_3u_9-u_4u_8\right)f^3}{u_4}-\frac{\left(u_2u_{12}-u_4u_{10}+u_5u_9\right)f}{u_4}\right)G\\
&-\frac{\left(u_3u_{12}-u_4u_{11}\right)f^2}{u_4}-\frac{u_5u_{12}}{u_4}=0
\end{aligned} \tag{23}$$

To simplify the calculations, create a relationship $G = \lambda f$ and using Eq. (23) we obtain the following definition

$$\lambda=-\frac{u_3u_{12}-u_4u_{11}}{u_2u_{12}-u_4u_{10}+u_5u_9}. \tag{24}$$

Substitution of Eq. (24) into Eq. (21) the axial load can be expressed as follows

$$T=-\frac{f^4A^2u_1+f^2Au_2+f^2u_3+u_5}{u_4}. \tag{25}$$

Eq. (25) is the main equation used to investigate the nonlinear buckling and post-buckling behavior of the FG-CNTRC truncated conical shells resting on elastic foundations under axial load.

3. Numerical results and discussion

3.1 Validation

In order to evaluate the reliability of the method used in this paper, the comparison of axial buckling load T_{cr} (kN) is made with results of the study (Ansari and Torabi 2016, Duc *et al*. 2017). Table 1 shows the comparison of critical buckling load T_{cr} (kN) of FG-Λ CNTRC truncated conical shells and Table 2 shows the comparison of critical buckling load T_{cr} (kN) of CNTRC truncated conical shells with various types of CNT reinforcements. The geometrical parameters and material properties of CNTRC truncated conical shells in these tables E_{11}^{CNT} = 5.6466 TPa, E_{22}^{CNT} = 7.0800 TPa, G_{12}^{CNT} = 1.9445 TPa, v_{12}^{CNT} = 0.175, v_m = 0.34, E_m = 2.5 GPa, h = 0.002m, R_1/h = 25. The results in these tables show a good agreement in this comparison.

3.2 Nonlinear buckling and post-buckling of FG-CNTRC truncated conical shells

In this section, nonlinear buckling and post-buckling analysis of FG-CNTRC truncated conical shells

Table 1 Comparison of critical buckling load T_{cr} (kN) of FG-Λ CNTRC truncated conical shells (h = 0.002 m, R_1/h = 25)

V^*_{CNT}		L/R_1 = 1			L/R_1 = 3		
		γ = 15°	γ = 30°	γ = 45°	γ = 15°	γ = 30°	γ = 45°
0.12	Duc *et al*. (2017)	79.62 (14,1)*	67.92 (1,2)	52.43 (18,1)	62.12 (1,4)	50.21 (1,3)	31.99 (10,1)
	Ansari and Torabi (2016)	79.72	69.88	54.67	61.68	48.91	33.40
	Present	79.83 (1,48)	69.78 (5,18)	54.25 (2,17)	61.52 (9,16)	48.37 (9,30)	33.85 (11,33)
0.17	Duc *et al*. (2017)	120.99 (1,3)	108.21 (10,1)	83.63 (18,1)	103,12 (7,1)	83.75 (1,2)	53.26 (14,1)
	Ansari and Torabi (2016)	123.56	107.10	82.75	102.59	80.85	54.76
	Present	124.22 (2,14)	106.42 (2,18)	82.16 (2,18)	102.29 (7,23)	80.10 (9,37)	54.02 (11,36)
0.28	Duc *et al*. (2017)	173.11 (10,1)	152.16 (14.1)	122.14 (10,1)	125.39 (1,2)	103.03 (1,3)	71.09 (14,1)
	Ansari and Torabi (2016)	173.25	153.36	121.34	127.76	102.19	70.32
	Present	172.81 (9,27)	153.13 (3,13)	121.73 (2,16)	127.35 (9,15)	102.21 (8,34)	70.89 (9,39)

* Buckling mode of the FG-CNTRC truncated conical shell

Table 2 Comparison of critical buckling load T_{cr} (kN) of CNTRC truncated conical shells (h = 0.002 m, R_1/h = 25, L/R_1 = 1)

Type	γ	V^*_{CNT} = 0.12		V^*_{CNT} = 0.17		V^*_{CNT} = 0.28	
		Ansari and Torabi (2016)	Present	Ansari and Torabi (2016)	Present	Ansari and Torabi (2016)	Present
UD	15°	98.46	98.94 (2,20)	152.01	152.68 (2,22)	231.34	231.78 (2,20)
	30°	88.32	88.23 (7,29)	135.20	135.96 (2,32)	193.55	192.20 (2,26)
	45°	70.91	70.43 (2,31)	107.10	107.18 (2,33)	157.23	157.03 (2,29)
FG-O	15°	67.08	68.19 (2,29)	104.52	103.70 (2,30)	145.49	144.94 (2,28)
	30°	57.55	57.52 (2,36)	88.56	87.72 (2,37)	126.28	126.67 (2,38)
	45°	43.99	43.17 (2,35)	66.68	66.83 (2,37)	97.82	97.69 (2,38)

subjected to axial load are presented. Poly (Methyl methacrylate) (PMMA) is considered as the matrix with material properties at room temperature The (10,10) single walled carbon nanotubes (SWCNTs) is considered as reinforce-ment. The material properties at room temperature of SWCNTs are given E_{11}^{CNT} = 5.6466 TPa, E_{22}^{CNT} = 7.0800 TPa, G_{12}^{CNT} = 1.9445 TPa, v_{12}^{CNT} = 0.175.

Figs. 3 and 4 illustrate the effect of CNT volume fraction of fibers and ratio R_1/h on the critical buckling load of CNTRC truncated conical shells. Three values of volume fraction are considered. It can be seen from these figures that the value of critical buckling load increases when the CNT volume fraction increases and vice versa. The CNT volume fraction increase results in load capacity of CNTRC truncated conical shells become a better because the elastic modulus of the CNT is significantly stronger than the elastic modulus of the matrix. It is clear that the ratio R_1/h has a substantial effect on the critical buckling load because the R_1/h increase makes the CNTRC truncated conical shells thinner results in the critical buckling load of the CNTRC truncated conical shells become lower. The critical buckling of FG-X CNTRC truncated conical shell is substantially higher than CNTRC truncated conical shell with uniform distribution type under conditions the same geometrical parameters. For instance, with the same geometrical parameters and V^*_{CNT} = 0.28, R_1/h = 100 the value of critical buckling load of FG-X CNTRC truncated conical shell is $T_{cr} \approx 7$ kN (Fig. 3) and the value of critical buckling load of CNTRC truncated conical shell with uniform distribution type is $T_{cr} \approx 5$ kN (Fig. 4).

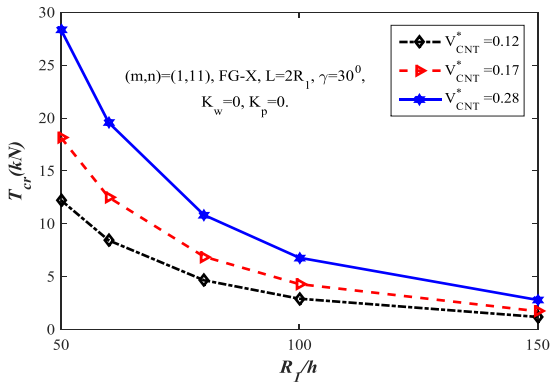

Fig. 3 Effect of CNT volume fraction and ratio R_1/h on the critical buckling load of truncated conical shells with FG-X reinforcement

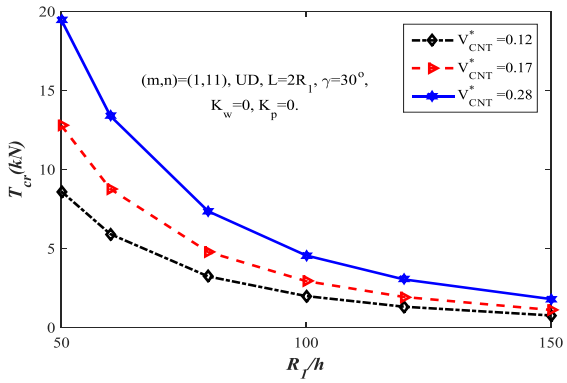

Fig. 4 Effect of CNT volume fraction and ratio R_1/h on the critical buckling load of truncated conical shells UD reinforcement

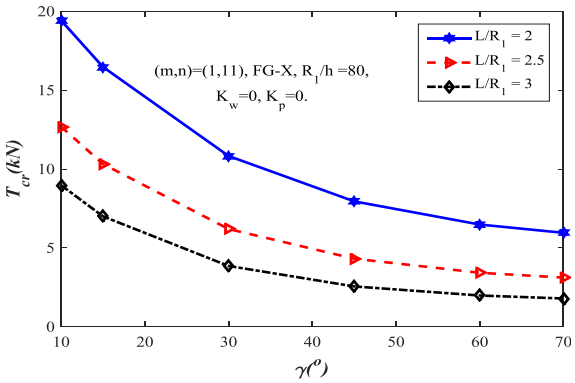

Fig. 5 Effect of semi vertex angle and ratio L/R_1 on the critical buckling load of FG-CNTRC truncated conical shells

Table 3 Effect of CNT volume fraction and ratio L/R_1 on the critical buckling load T_{cr} (kN) of FG-CNTRC truncated conical shells

L/R_1	V^*_{CNT} = 0.12	V^*_{CNT} = 0.17	V^*_{CNT} = 0.28
1	21.665	31.639	51.179
2	4.652	6.886	10.828
3	1.680	2.515	3.856

Fig. 5 depicts the effect of semi vertex angle on the critical buckling load of FG-CNTRC truncated conical shells under three different sets of length to radius ratio (L / R_1). It is clear that the value of the critical buckling load of FG-CNTRC truncated conical shells decreases when the value of semi vertex angles increases.

Table 3 compares the critical buckling load of FG-CNTRC truncated conical shells with three different values of CNT volume fractions and length to radius ratio (L/R_1). The geometrical parameters of the truncated conical shells are (n, m) = (1, 11), FG-X, R_1/h = 80, γ = 30°, K_w = 0, K_p = 0. Clearly, the lower the length to small radius ratio (L / R_1), the higher the value of the critical buckling load of FG-CNTRC truncated conical shells in both of Fig. 5 and Table 3.

Table 4 presents the effect of three different CNT volume fractions and various types of CNT reinforcements on the critical buckling load of FG-CNTRC truncated conical shells. The geometrical parameters of the truncated conical shells are (n, m) = (1, 11), L/R_1 = 1, R_1/h = 80, γ = 30°, K_w = 0, K_p = 0. It is noticeable that the value of critical buckling load is affected by various types of CNT reinforcements. The value of critical buckling load of FG-X CNTRC is the highest and FG-O CNTRC is the lowest. For instance, in the case V^*_{CNT}= 0.12 the value of the critical buckling load of FG-X CNTRC truncated conical shell is T_{cr} = 21.665 kN, this value is dramatically decreased for FG-O CNTRC truncated conical shell (T_{cr} = 7.592 kN).

Table 5 compares the critical buckling load of CNTRC truncated conical shells resting on elastic foundations with various types of CNT reinforcements in three cases of CNT volume fraction. The geometrical parameters of the truncated conical shells are (n, m) = (1, 11), L/R_1 = 1, R_1/h = 80, γ = 30°, K_w = 5×10^5 N/m^3, K_p = 1×10^4 N/m. It is clear that the critical buckling load of FG-X CNTRC truncated conical shells with V^*_{CNT} = 0.28 is the highest and the critical buckling load of FG-O CNTRC truncated conical shells with V^*_{CNT}= 0.12 is the lowest. It is understood that among the various types of CNT reinforcements the FG-X

Table 4 Effect of CNT volume fraction and various types of CNT reinforcements on the critical buckling load T_{cr} (kN) of FG-CNTRC truncated conical shells

Type	V^*_{CNT} = 0.12	V^*_{CNT} = 0.17	V^*_{CNT} = 0.28
FG-X	21.665	31.639	51.179
FG-O	7.592	10.940	17.229
FG-Λ	15.288	22.226	35.462

Table 5 Effect of CNT volume fraction and various types of CNT reinforcements on the critical buckling load T_{cr} (kN) of FG-CNTRC truncated conical shells resting on elastic foundations

Type	V^*_{CNT} = 0.12	V^*_{CNT} = 0.17	V^*_{CNT} = 0.28
FG-X	23.536	33.510	53.050
FG-O	9.463	12.810	19.100
FG-Λ	17.159	24.097	37.333

type makes the load capacity of the CNTRC truncated conical shells is the best. From Tables 4 and 5, the value of the critical buckling load of FG-CNTRC truncated conical shells resting on elastic foundations is higher than the FG-CNTRC truncated conical shells without the elastic foundations.

Figs. 6 and 7 compare the effect of small radius to thickness ratio (R_1/h) on the post-buckling behavior of FG-X (Fig. 6) and UD (Fig. 7) CNTRC truncated conical shells with the same geometrical parameters. Three cases of small radius to thickness ratio R_1/h = (60, 80, 100) are consirded. It is found that when R_1/h ratio is increased, the post-buckling load – deflection curve becomes lower and vice versa. The post-buckling curve shows the post-buckling strength of CNTRC truncated conical shells. In other words, R_1/h increase makes the CNTRC truncated conical shells thinner which results in the lower the load capacity of the FG-CNTRC truncated conical shells. The results show that the post-buckling curve of FG-X CNTRC truncated conical shell is lower than UD CNTRC truncated conical shell under the same conditions and the deflection of the shells is not sufficiently large.

Fig. 8 shows the influence of length to small radius ratio (L/R_1) on the post-buckling behavior of FG-CNTRC truncated conical shells. Three value different of length to small radius ratio (L/R_1) are considered. It is noticeable that when L/R_1 increases, the post-buckling curve is lower and vice versa. That is correct because L/R_1 increase makes the CNTRC truncated conical shells becomes thinner and the load capacity is decreased. This figure shows that the post-buckling curve is substantially decreased when L/R_1 ratio increases form L/R_1 = 1 to L/R_1 = 2. In contrast, the post-buckling curve is slightly decreased with the value of L/R_1 ratio more than L/R_1 = 2.

Fig. 9 presents the influence of semi vertex angle γ on

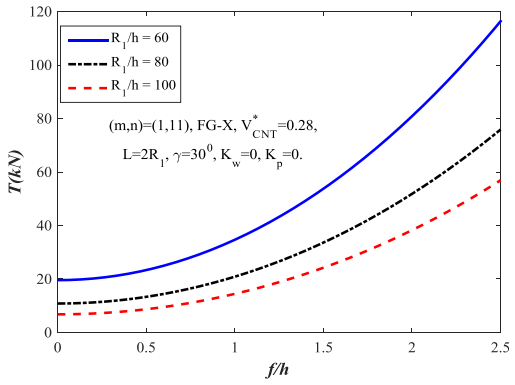

Fig. 6 Effect of ratio R_1/h on the post-buckling curves of FG-X CNTRC truncated conical shells

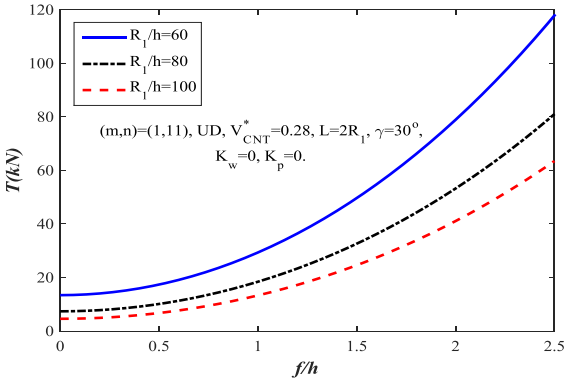

Fig. 7 Effect of ratio R_1/h on the post-buckling curves of CNTRC truncated conical shells with UD type

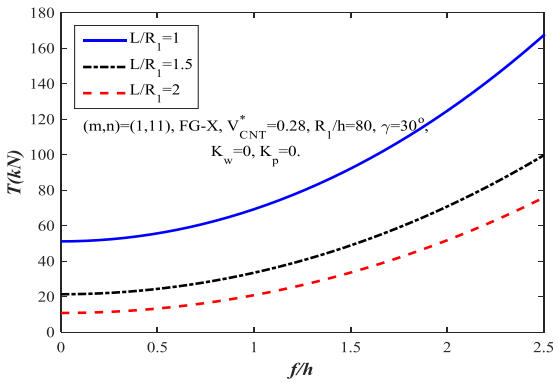

Fig. 8 Effect of ratio L/R_1 on the post-buckling curves of FG-CNTRC truncated conical shells

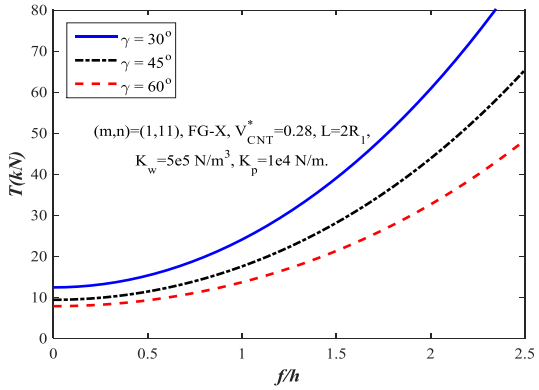

Fig. 9 Effect of semi vertex angle γ on the post-buckling curves of FG-CNTRC truncated conical shells resting on elastic foundations

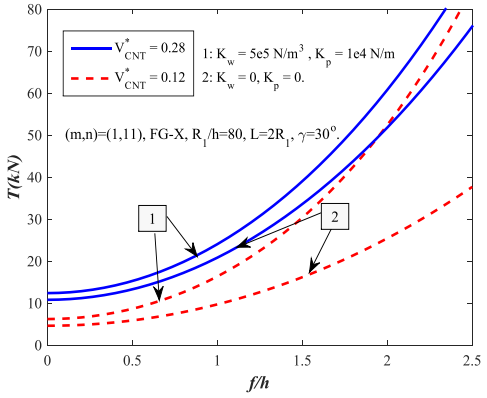

Fig. 10 Effect of volume fraction of fibers on the post-buckling curves of FG-CNTRC truncated conical shells resting on elastic foundations

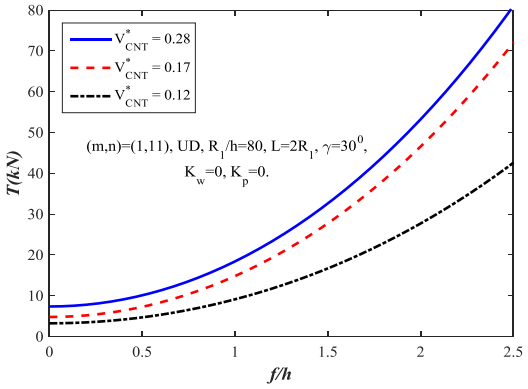

Fig. 11 Effect of volume fraction of fibers on the post-buckling curves of CNTRC truncated conical shells with uniform distribution type

the post-buckling behavior of FG-CNTRC truncated conical shells. Three different values of semi vertex angles are considered. The results in this figure show that increasing the value of the semi vertex angles leads to the post-buckling curve of the FG-CNTRC truncated conical shells is lower.

Fig. 10 compares the post-buckling behavior of FG-CNTRC truncated conical shell resting on the elastic foundation and the FG-CNTRC truncated conical shell without the elastic foundation. The geometrical parameters are shown in Fig. 10. It is clear that the elastic foundation has considerably affected help the capacity load of FG-CNTRC truncated conical shells is better.

Fig. 11 illustrates the effect of CNT volume fraction of fibers on the post-buckling behavior of CNTRC truncated conical shells with uniform distribution type. Three different sets of CNT volume fraction V_{CNT}^{*} = (0.12, 0.17, 0.28) are considered. It can be seen that the post-buckling curve is higher when CNT volume fraction of fibers increases and vice versa. That is understood that the CNT volume fraction of fibers increase results in the CNTRC truncated conical shells have the better post-buckling strength because the elastic modulus of the carbon nanotubes is significantly stronger than the elastic modulus of the matrix.

4. Conclusions

By using the approximate solution about the form of two-component deflection function and the superposition method, the present study aims to analysis the nonlinear buckling and post-buckling behaviors of FG-CNTRC truncated conical shells subjected to axial load and resting on elastic foundations. The main equations are obtained by Galerkin method and Airy stress function method based on the classical theory. The effect of geometrical parameters, both FG and UD types of CNT, nanotube volume fraction, elastic foundations on the static analysis of FG-CNTRC truncated conical shells are investigated. Some conclusions can be obtained from this study:

- The critical buckling load and post-buckling strength of FG-CNTRC truncated conical shells are significantly effected by various types of CNTs distributions. The critical buckling load and post-buckling strength of FG-X CNTRC truncated conical shells is the highest.
- CNT volume fraction of fibers has a substantial effect on the critical buckling load and post-buckling curves.
- The elastic foundations affected on the nonlinear buckling and post-buckling behaviors of FG-CNTRC truncated conical shells. In addition, the effect of Pasternak elastic foundation is stronger than Winkler elastic foundation.
- The geometrical parameters have influences on the value of critical buckling load and post-buckling curves of FG-CNTRC truncated conical shells.

Acknowledgments

This work has been supported by Vietnam National University, Hanoi (VNU), under Project No. QG.18.37. The authors are grateful for this support.

Conflict of interest statement

The authors declare no conflict of interest.

References

Akbari, M., Kiani, Y. and Eslami, M.R. (2015), "Thermal buckling of temperature-dependent FGM conical shells with arbitrary edge supports", *Acta. Mech.*, **226**(3), 897-915.

Ansari, R. and Torabi, J. (2016), "Numerical study on the buckling and vibration of functionally graded carbon nanotube-reinforced composite conical shells under axial loading", *Compos. Part B Eng.*, **95**, 196-208.

Chan, D.Q., Dung, D.V. and Hoa, L.K. (2018), "Thermal buckling analysis of stiffened FGM truncated conical shells resting on elastic foundations using FSDT", *Acta. Mech.* **229**(5), 2221-2249.

Duc, N.D. and Cong, P.H. (2015), "Nonlinear thermal stability of eccentrically stiffened functionally graded truncated conical shells surrounded on elastic foundations", *Euro. J. Mech. A Solids.*, **50**, 120-131.

Duc, N.D. and Nguyen, P.D. (2017), "The dynamic response and vibration of functionally graded carbon nanotubes reinforced composite (FG-CNTRC) truncated conical shells resting on elastic foundation", *Materials*, **10**(10), 1194.

Duc, N.D., Cong, P.H., Tuan, N.D., Phuong, T. and Thanh, N.V. (2017), "Thermal and mechanical stability of functionally graded carbon nanotubes (FG CNT) reinforced composite truncated conical shells surrounded by the elastic foundations", *Thin-Wall. Struct.*, **115**, 300-310.

Duc, N.D., Kim, S.E. and Chan, D.Q. (2018), "Thermal buckling analysis of FGM sandwich truncated conical shells reinforced by FGM stiffeners resting on elastic foundations using FSDT", *J. Therm. Stress*, **41**(3), 331-365.

Dung, D.V., Hoai, B.T.T. and Hoa, L.K. (2017), "Postbuckling nonlinear analysis of FGM truncated conical shells reinforced by orthogonal stiffeners resting on elastic foundations", *Acta Mech.*, **228**(4), 1457-1479.

Heydarpour, Y., Aghdam, M.M. and Malekzadeh, P. (2014), "Free vibration analysis of rotating functionally graded carbon

nanotube-reinforced composite truncated conical shells", *Compos. Struct.*, **117**, 187-200.
Hu, H.T. and Chen, H.C. (2018), "Buckling optimization of laminated truncated conical shells subjected to external hydrostatic compression", *Compos. Part B Eng.*, **135**, 95-109.
Jam, J.E. and Kiani, Y. (2016), "Buckling of pressurized functionally graded carbon nanotube reinforced conical shells", *Compos. Struct.*, **125**, 586-595.
Kamarian, S., Salim, M., Dimitri, R. and Tornabene, F. (2016), "Free vibration analysis of CNTRC conical shells based on first-order shear deformation theory", *Int. J. Mech. Sci.*, **108-109**, 157-165.
Khayat, M., Poorveis, D. and Moradi, S. (2017), "Buckling analysis of functionally graded truncated conical shells under external displacement-dependent pressure", *Steel Comp. Struct., Int. J.*, **23**(1), 1-6.
Mehri, M., Asadi, H. and Wang, Q. (2016a), "Buckling and vibration analysis of a pressurized CNT reinforced functionally graded truncated conical shell under an axial compression using HDQ method", *Comput. Methods. Appl. Mech. Eng.*, **303**, 75-100.
Mehri, M., Asadi, H. and Wang, Q. (2016b), "On dynamic instability of a pressurized functionally graded carbon nanotube reinforced truncated conical shell subjected to yawed supersonic airflow", *Compos. Struct.*, **153**, 938-951.
Mirzaei, M. and Kiani, Y. (2015), "Thermal buckling of temperature dependent FG-CNT reinforced composite conical shells", *Aerosp. Sci. Technol.*, **47**, 42-53.
Morozov, E.V., Lopatin, A.V. and Nesterov, V.A. (2011), "Buckling analysis and design of anisogrid composite lattice conical shells", *Compos. Struct.*, **93**(12), 3150-3162.
Naj, R., Boroujerdy, M.S. and Eslami, M.R. (2008), "Thermal and mechanical instability of functionally graded truncated conical shells", *Thin-Wall. Struct.*, **46**, 65-78.
Najafov, A.M. and Sofiyev, A.H. (2013), "The non-linear dynamics of FGM truncated conical shells surrounded by an elastic medium", *Int. J. Mechan. Sci.*, **66**, 33-44.
Seidi, J., Khalili, S.M.R. and Malekzadeh, K. (2015), "Temperature-dependent buckling analysis of sandwich conical shell with thin functionally graded facesheets", *Compos. Struct.*, **131**, 682-691.
Shadmehri, F., Hoa, V.S. and Hojjati, M. (2012), "Buckling of conical composite shells", *Compos. Struct.*, **94**, 787-792.
Sharghi, H., Shakouri, M. and Kouchakzadeh, M.A. (2016), "An analytical approach for buckling analysis of generally laminated conical shells under axial compression", *Acta Mech.*, **227**(4), 1181-1198.
Shen, H.S. (2009), "Nonlinear bending of functionally graded carbon nanotube reinforced composite plates in thermal environments", *Compos. Struct.*, **91**, 9-19.
Sofiyev, A.H. (2010), "The buckling of FGM truncated conical shells subjected to axial compressive load and resting on Winkler-Pasternak foundations", *Int. J. Press. Vesels Pip.*, **87**, 753-761.
Sofiyev, A.H. (2011), "Influence of the initial imperfection on the non-linear buckling response of FGM truncated conical shells", *Int. J. Mech. Sci.*, **53**(9), 753-761.
Sofiyev, A.H. (2013), "On the vibration and stability of shear deformable FGM truncated conical shells subjected to an axial load", *Compos. Part B Eng.*, **80**, 53-62.
Sofiyev, A.H. and Kuruoglu, N. (2013), "Buckling analysis of nonhomogeneous orthotropic thin-walled truncated conical shells in large deformation", *Thin-Wall. Struct.*, **62**, 131-141.
Sofiyev, A.H. and Kuruoglu, N. (2015), "Buckling of non-homogeneous orthotropic conical shells subjected to combined load", **19**(1), 1-19.
Sofiyev, A.H. and Kuruoglu, N. (2016), "The stability of FGM truncated conical shells under combined axial and external mechanical loads in the framework of the shear deformation theory", *Compos. Part B Eng.*, **92**, 463-476.
Sofiyev, A.H. and Schnack, E. (2003), "The buckling of cross-ply laminated non-homogeneous orthotropic composite conical thin shells under a dynamic external pressure", *Acta Mech.*, **162**(1-4), 29-40.
Sofiyev, A.H., Zerin, Z., Allahverdiev P.B., Hui, D., Turan, F. and Erdem, H. (2017), "The dynamic instability of FG orthotropic conical shells within the SDT", *Steel Compos. Struct., Int. J.*, **25**(5), 581-591.
Topal, U. (2013), "Pareto optimum design of laminated composite truncated circular conical shells", *Steel Compos. Struct., Int. J.*, **14**(4), 397-408.
Torabi, J., Kiani, Y. and Eslami, M.R. (2013), "Linear thermal buckling analysis of truncated hybrid FGM conical shells", *Compos. Part B Eng.*, **50**, 265-272.
Viola, E., Rossetti, L., Fantuzzi, N. and Tornabene, F. (2014), "Static analysis of functionally graded conical shells and panels using the generalized unconstrained third order theory coupled with the stress recovery", *Compos. Struct.*, **112**, 44-65.
Zielnica, J. (2012), "Buckling and stability of elastic-plastic sandwich conical shells", *Steel Compos. Struct., Int. J.*, **13**(2), 157-169.

CC

Appendix I

$$H_{11}(F_1)= c_{12}e^{2x}\frac{\partial^4 F_1}{\partial x^4}+(c_{11}+4c_{12}-c_{22})e^{2x}\frac{{}^3F_1}{x^3}$$
$$+(5c_{12}+3(c_{11}-c_{22})-c_{21})e^{2x}\frac{\partial^3 F_1}{\partial x^2}+(c_{11}+c_{22}-2c_{31})e^{2x}\frac{{}^4F_1}{x^2?\varphi^2}$$
$$+(c_{11}+3c_{22}-4c_{31})e^{2x}\frac{\partial^3 F_1}{\partial x\ \varphi^2}+(2c_{22}-2c_{31}+2c_{21})e^{2x}\frac{{}^2F_1}{?\varphi^2}$$
$$+(2c_{12}+2c_{11}-2c_{22}-2c_{21})e^{2x}\frac{\partial^2 F_1}{\partial x}+c_{21}e^{2x}\frac{{}^4F_1}{\varphi^4}$$
$$-S_1e^{3x}\left(\frac{\partial^2 F_1}{\partial x^2}+3\frac{\partial F_1}{\partial x}+2F_1\right)\cot\gamma,$$

$$H_{12}(w)= c_{13}\frac{\partial^4 w}{\partial x^4}+(-4c_{13}-c_{23}+c_{14})\frac{{}^3w}{x^3}$$
$$+(5c_{13}+3(c_{23}-c_{14})-c_{24})\frac{\partial^3 w}{\partial x^2}+(-2c_{13}+2(c_{14}-c_{23})+2c_{24})\frac{w}{x}$$
$$-(3c_{14}+4c_{32}+c_{23})\frac{\partial^3 w}{\partial x\ \varphi^2}+(c_{14}+2c_{32}+c_{23})\frac{{}^4w}{\partial x^2\ \varphi^2}$$
$$+(2c_{14}-2c_{32}+2c_{24})\left(\frac{\partial^3 w}{\partial x\partial\varphi^2}+\frac{\partial^2 w}{\partial x^2}\right)+c_{24}\frac{\partial^4 w}{\partial\varphi^4}-S_1^4e^{4x}K_w w$$
$$+S_1^2e^{2x}K_p\left(\frac{\partial^2 w}{\partial x^2}+\frac{{}^2w}{\varphi^2}\right)$$

$$H_{13}(F_1,w)= e^{2x}\left(\frac{\partial^3 F_1}{\partial x^2}+3\frac{F_1}{x}+2F_1\right)\left(\frac{\partial^2 w}{\partial x^2}+\frac{{}^2w}{\varphi^2}\right)$$
$$+e^{2x}\left(\frac{\partial^3 F_1}{\partial\varphi^2}+\frac{F_1}{x}+2F_1\right)\left(\frac{\partial^2 w}{\partial x^2}-\frac{w}{x}\right)$$
$$+2e^{2x}\left(\frac{\partial^3 F_1}{\partial x\ \varphi}+\frac{F_1}{\partial\varphi}\right)\left(\frac{\partial^2 w}{\partial\varphi}-\frac{{}^2w}{\partial x\ \varphi}\right),$$

$$H_{21}(F_1)= A_{11}^*e^{2x}\frac{\partial^4 F_1}{\partial x^4}+4A_{11}^*e^{2x}\frac{{}^3F_1}{x^3}+(5A_{11}^*-A_{22}^*)e^{2x}\frac{?^2F_1}{?x^2}$$
$$+(2A_{11}^*-2A_{22}^*)e^{2x}\frac{\partial^3 F_1}{\partial x}++(2A_{66}^*-4A_{12}^*)e^{2x}\frac{{}^3F_1}{x?\varphi^2}$$
$$+(2A_{22}^*-2A_{12}^*+A_{66}^*)e^{2x}\frac{\partial^3 F_1}{\partial\varphi^2}+A_{22}^*e^{2x}\frac{{}^4F_1}{\varphi^4},$$

$$H_{22}(w)= c_{12}\frac{\partial^4 w}{\partial x^4}+(c_{22}-c_{11}-4c_{12})\frac{{}^3w}{x^3}+(5c_{12}-3c_{22}+3c_{11}-c_{21})\frac{?^2w}{?x^2}$$
$$+(-2c_{12}+2c_{22}-2c_{11}+2c_{21})\frac{\partial^3 w}{\partial x}+(-3c_{22}+4c_{31}-c_{11})\frac{{}^3w}{x?\varphi^2}$$
$$+(c_{11}+c_{22}-2c_{31})\frac{\partial^3 w}{\partial x^2\ \varphi^2}+(2c_{22}+2c_{21}-2c_{31})\frac{{}^2w}{\partial\varphi^2}+c_{12}\frac{?^4w}{\varphi^4}$$
$$+S_1e^x\cot\gamma\left(\frac{\partial^2 w}{\partial x^2}-\frac{w}{x}\right)$$

$$H_{23}(w,w)= -\left(\frac{\partial^2 w}{\partial\varphi}\right)^2+2\frac{w}{\varphi}\frac{\partial^3 w}{\partial x\ \varphi}+\frac{\partial^2 w}{\partial x^2}-\frac{\partial w}{x}\frac{{}^2w}{?\varphi^2}$$
$$-\left(\frac{\partial^2 w}{\partial x\ \varphi}\right)^2+\frac{\partial^2 w}{\partial x^2}-\frac{\partial w}{x}\frac{w}{?x}.$$

Appendix II

$$a_1=\left(8A_{11}^*m_1^4-16m_2^2A_{12}^*m_1^2+8A_{22}^*m_2^4+8m_2^2A_{66}^*m_1^2\right)\Big/\left(10A_{11}^*m_1^2+4A_{12}^*m_2^2+2A_{22}^*m_1^2-4A_{66}^*m_2^2-2A_{66}^*m_2^2\right)$$
$$a_2=\left(-16A_{11}^*m_1^3+16A_{12}^*m_1m_2^2-8A_{66}^*m_1m_2^2+2A_{11}^*m_1-2A_{22}^*m_1\right),$$
$$a_3=\frac{1}{8}m_1-\frac{1}{8}m_1^3-\frac{1}{8}m_1m_2^2,\ a_4=\left(256A_{11}^*m_1^4-80A_{11}^*m_1^2+16A_{22}^*m_1^2\right),$$
$$a_5=\left(-256A_{11}^*m_1^3+8A_{11}^*m_1-8A_{22}^*m_1\right),a_6=\left(m_1^3-\frac{1}{4}m_1\right.$$
$$a_7=\left(16A_{22}^*m_2^4+8A_{12}^*m_2^2-8A_{22}^*m_2^2-4A_{66}^*m_2^2\right),$$
$$a_8=\left(-54A_{11}^*m_1^3+6A_{12}^*m_1m_2^2-3A_{66}^*m_1m_2^2+3A_{11}^*m_1-3A_{22}^*m_1\right),$$
$$a_9=\frac{1}{2}\left(2A_{22}^*m_2^2-2A_{12}^*m_2^2+45A_{11}^*m_1^2-9A_{22}^*m_1^2-81A_{11}^*m_1^4\right)\Big/\left(A_{22}^*m_2^4+A_{66}^*m_2^2+18m_2^2A_{12}^*m_1^2-9m_2^2A_{66}^*m_1^2\right)$$
$$a_{10}=\left(\frac{9}{8}m_1^2+\frac{1}{2}m_1^2m_2^2\right),a_{11}=\left(\frac{3}{4}m_1^3-\frac{3}{8}m_1+\frac{1}{4}m_1m_2^2\right)$$
$$a_{12}=\left(16A_{11}^*m_1^4+4A_{11}^*m_1^2+4A_{22}^*m_1^2+A_{22}^*\right),$$
$$a_{13}=m_1\left(16c_{12}m_1^2-4c_{11}m_1^2-16c_{12}m_1^2\right)\Big/\left(4c_{22}m_1^2-4c_{12}-c_{11}+3c_{12}+c_{22}\right)$$
$$a_{14}=\left(8c_{12}m_1^4-12c_{12}m_1^2+14c_{12}m_1^2+2c_{21}m_1^2+\frac{1}{2}c_{12}+\frac{1}{2}c_{21}\right)$$
$$a_{15}=\left(16A_{11}^*m_1^4-20A_{11}^*m_1^2+4A_{22}^*m_1^2\right),$$
$$a_{16}=\left(32A_{11}^*m_1^3-4A_{11}^*m_1+4A_{22}^*m_1\right),a_{17}=\left(\frac{1}{2}m_1^2-\frac{1}{2}m_1^2m_2^2\right)$$
$$a_{18}=\left(\frac{1}{4}m_1m_2^2+\frac{1}{4}m_1-\frac{1}{4}m_1^3\right)$$
$$a_{21}=\left(\frac{1}{2}m_1^2m_2^2-\frac{3}{8}m_1^2\right),a_{22}=\left(\frac{3}{8}m_1-\frac{1}{4}m_1m_2^2+\frac{1}{4}m_1^3\right.?,$$
$$a_{23}=\frac{1}{2}\left(2A_{22}^*+A_{22}^*m_2^4+A_{11}^*m_1^2+A_{22}^*m_1^2+A_{11}^*m_1^4\right)\Big/\left(-2m_2^2A_{22}^*+m_2^2A_{66}^*m_1^2-2m_2^2A_{12}^*m_1^2\right)$$
$$a_{19}=\left(2A_{11}^*m_1^3-2A_{12}^*m_1m_2^2+A_{66}^*m_1m_2^2-A_{11}^*m_1+A_{22}^*m_1\right),$$
$$a_{20}=\frac{1}{2}\left(2A_{22}^*m_2^2-5A_{11}^*m_1^2+A_{11}^*m_1^4+2A_{12}^*m_2^2+A_{s22}m_2^4\right)\Big/\left(A_{22}^*m_1^2-A_{66}^*m_2^2-2m_2^2A_{12}^*m_1^2+m_2^2A_{66}^*m_1^2\right)$$
$$a_{24}=\frac{1}{2}\left(c_{12}m_1^4-2m_2^2c_{21}+7c_{12}m_1^2-6c_{12}m_1^2+c_{21}m_2^4+8m_2^2c_{31}\right.\Big/\left.+c_{11}m_1^2m_2^2+c_{22}m_1^2m_2^2-2c_{31}m_1^2m_2^2+c_{21}m_1^2+c_{21}+c_{12}\right)$$
$$a_{25}=\frac{1}{2}\left(c_{22}m_1m_2^2+8c_{31}m_1m_2^2-c_{11}m_1m_2^2+c_{11}m_1^3-c_{22}m_1\right.\Big/\left.3c_{12}m_1+4c_{12}m_1^3+c_{11}m_1-4c_{12}m_1^3+4c_{12}m_1-c_{22}m_1^3\right)$$

Appendix III

$$u_1 = \frac{\pi^2 m \sin(\gamma)\left(-1+\mathrm{e}^{4x_0}\right)u_1^c}{8\left(9\pi^2m^2+4x_0^2\right)\left(\pi^2m^2+x_0^2\right)\left(\pi^2m^2+4x_0^2\right)},$$

$$u_1^c = \begin{cases} 16b_7x_0^5 - 16b_6x_0^5 - 16b_5x_0^5 + 6\pi^4b_5m^4x_0 + 18\pi^4b_6m^4x_0 \\ +5\pi^3b_1m^3x_0^2 + 54\pi^3b_2m^3x_0^2 + 26\pi^3b_3m^3x_0^2 - 5\pi^3b_4m^3x_0^2 \\ -28\pi^2b_6m^2x_0^3 - 52\pi^2b_7m^2x_0^3 + 20\pi b_1mx_0^4 + 24\pi b_2mx_0^4 \\ +8\pi b_3mx_0^4 - 20\pi b_4mx_0^4 + 18\pi^5b_3m^5 + 20\pi^2b_5m^2x_0^3 \\ 36\pi^4b_7m^4x_0 \end{cases}$$

$$u_2 = \frac{2\pi^2 m \sin(\gamma)\left(-1+\mathrm{e}^{3x_0}\right)u_2^{c1}}{3\left(4\pi^2m^2+9x_0^2\right)\left(16\pi^2m^2+9x_0^2\right)} + \frac{\pi^2 m \sin(\gamma)\left(-1+\mathrm{e}^{4x_0}\right)u_2^{c2}}{4\left(\pi^2m^2+x_0^2\right)\left(\pi^2m^2+4x_0^2\right)},$$

$$u_2^{c1} = \begin{cases} 32b_{33}m^3\pi^3 - 48\pi^2m^2b_{37}x_0 + 24\pi^2m^2b_{35}x_0 + 18\pi mb_{33}x_0^2 \\ 54\pi mb_{31}x_0^2 - 27b_{37}x_0^3 - 27b_{35}x_0^3 \end{cases}$$

$$u_2^{c2} = \begin{cases} \pi^3b_{34}m^3 - 2\pi^2m^2b_{38}x_0 + \pi^2m^2b_{36}x_0 + 3\pi mb_{32}x_0^2 \\ \pi mb_{34}x_0^2 - 2b_{38}x_0^3 - 2b_{36}x_0^3 \end{cases}$$

$$u_3 = \frac{\pi^2 m\left(-1+\mathrm{e}^{4x_0}\right)\sin(\gamma)u_3^c}{4\left(\pi^2m^2+x_0^2\right)\left(\pi^2m^2+4x_0^2\right)},$$

$$u_3^c = \begin{cases} \pi^2m^2b_{45}x_0 + \pi mb_{42}x_0^2 + 3\pi mb_{41}x_0^2 \\ -2b_{46}x_0^3 - 2\pi^2m^2b_{46}x_0 - 2b_{45}x_0^3 + \pi^3m^3b_{42} \end{cases}$$

$$u_4 = \frac{m^2\pi^3S_1^2}{24\left(\pi^2m^2+4x_0^2\right)}\left(\frac{\sin(\gamma)u_4^{c1}}{x_0^2} + \frac{3n^2u_4^{c2}}{\sin(\gamma)\left(9x_0^2+\pi^2m^2\right)}\right)$$

$$u_4^{c1} = \begin{cases} 7\pi^2m^2 + 4\mathrm{e}^{6x_0}\pi^2m^2 + 3\pi^2\mathrm{e}^{4x_0}m^2 + 16\mathrm{e}^{6x_0}x_0^2 \\ 9\mathrm{e}^{4x_0}x_0^2 - 25x_0^2 \end{cases}$$

$$u_4^{c2} = \begin{cases} 16\mathrm{e}^{6x_0}x_0^2 + 9\mathrm{e}^{4x_0}x_0^2 - 25x_0^2 - 5\pi^2m^2 + 4\mathrm{e}^{6x_0}\pi^2m^2 \\ +\pi^2\mathrm{e}^{4x_0}m^2 \end{cases}$$

$$u_5 = \begin{cases} \dfrac{(\pi b_{60}m - b_{63}x_0)\mathrm{e}^{2x_0}}{2\left(\pi^2m^2+x_0^2\right)} + \dfrac{2(2\pi b_{61}m - 3b_{64}x_0)\mathrm{e}^{3x_0}}{3\left(9x_0^2+4\pi^2m^2\right)} + \\ \dfrac{(\pi b_{62}m - 2b_{65}x_0)\mathrm{e}^{4x_0}}{4\left(\pi^2m^2+4x_0^2\right)} + \dfrac{S_1^4m\pi\left(1-\mathrm{e}^{6x_0}\right)K_w}{12\left(9x_0^2+\pi^2m^2\right)} \end{cases} m\pi^2\sin(\gamma)$$

$$u_8 = \frac{\pi^3m^2\sin(\gamma)u_8^c\left(-1+\mathrm{e}^{4x_0}\right)}{8\left(\pi^2m^2+x_0^2\right)\left(\pi^2m^2+4x_0^2\right)\left(9\pi^2m^2+4x_0^2\right)},$$

$$u_8^c = \begin{cases} 14\pi^2m^2b_{17}x_0^2 - 22\pi^2m^2b_{18}x_0^2 + 26\pi^2m^2b_{30}x_0^2 - 24\pi mb_{25}x_0^3 \\ -9\pi^4m^4b_{17} + 18\pi^4m^4b_{30} - 12\pi mb_{24}x_0^3 + 8b_{30}x_0^4 + 8b_{17}x_0^4 \\ 27\pi^3m^3b_{24}x_0 + 6\pi^3m^3b_{25}x_0 + 8b_{18}x_0^4 \end{cases}$$

$$u_9 = \frac{\sin(\gamma)S_1^2\pi^5m^4u_9^c}{48\left(\pi^2m^2+9x_0^2\right)\left(\pi^2m^2+x_0^2\right)\left(\pi^2m^2+4x_0^2\right)x_0^2}$$

$$u_9^c = \begin{cases} 12\mathrm{e}^{4x_0}\pi^4m^4 + 16\mathrm{e}^{6x_0}\pi^4m^4 + 111\mathrm{e}^{4x_0}\pi^2m^2x_0^2 + 80\mathrm{e}^{6x_0}\pi^2m^2x_0^2 \\ 64\mathrm{e}^{6x_0}x_0^4 - 191\pi^2m^2x_0^2 - 28\pi^4m^4 + 27\mathrm{e}^{4x_0}x_0^4 - 91x_0^4 \end{cases}$$

$$u_{10} = -\frac{m^2\pi^3\sin(\gamma)\left(1-\mathrm{e}^{2x_0}\right)u_{10}^{c1}}{4\left(x_0^2+m^2\pi^2\right)\left(x_0^2+4m^2\pi^2\right)} + \begin{cases} \dfrac{\left(\pi^2b_{37}m^2 + 3b_{40}x_0m\pi - 2b_{37}x_0^2\right)\left(1-\mathrm{e}^{4x_0}\right)}{8\left(4x_0^2+m^2\pi^2\right)\left(x_0^2+m^2\pi^2\right)} \\ -\dfrac{4\left(8\pi^2b_{36}m^2 + 18b_{39}x_0m\pi - 9b_{36}x_0^2\right)\mathrm{e}^{3x_0}}{3\left(9x_0^2+4m^2\pi^2\right)\left(9x_0^2+16m^2\pi^2\right)} \end{cases} m^2\pi^3\sin(\gamma)$$

$$u_{10}^c = \begin{cases} 4\pi^2c_{24}m^2 + 4\pi^2b_{35}m^2 - 8\pi^2K_{16}c_{21}m^2 + 6b_{38}x_0m\pi + c_{24}x_0^2 \\ 2b_{35}x_0^2 - 2K_{16}c_{21}x_0^2 \end{cases}$$

$$u_{11} = \frac{\pi^3m^2\sin(\gamma)u_{11}^{c1}\left(1-\mathrm{e}^{4x_0}\right)}{\left(32x_0^2+8m^2\pi^2\right)\left(x_0^2+m^2\pi^2\right)} + \frac{4\pi^3m^2\sin(\gamma)\left(1-\mathrm{e}^{3x_0}\right)u_{11}^{c2}}{\left(27x_0^2+48m^2\pi^2\right)\left(9x_0^2+4m^2\pi^2\right)},$$

$$u_{11}^{c1} = \left(\pi^2m^2b_{52} - 2\pi^2m^2b_{59} + 3b_{56}x_0m\pi - 2b_{59}x_0^2 - 2b_{52}x_0^2\right),$$

$$u_{11}^{c2} = \left(8m^2\pi^2b_{51} + 18b_{55}x_0m\pi - 9b_{51}x_0^2\right)$$

$$u_{12} = -\frac{16\pi^3m^2S_1^2\left(9x_0^2+m^2\pi^2\right)u_{12}^{c3}\sin(\gamma)}{5u_{12}^{c2}} + \frac{\pi^3m^2S_1^3\cos(\gamma)u_{12}^{c1}}{4u_{12}^{c2}},$$

$$u_{12}^{c1} = \left(25x_0^2+4m^2\pi^2\right)\begin{cases} 4\pi^2\mathrm{e}^{6x_0}m^2 + \pi^2m^2\mathrm{e}^{4x_0} - 5m^2\pi^2 \\ 25x_0^2 + 9\mathrm{e}^{4x_0}x_0^2 + 16\mathrm{e}^{6x_0}x_0^2 \end{cases}$$

$$u_{12}^{c2} = \left(4\pi^6m^6 + 77\pi^4m^4x_0^2 + 469m^2\pi^2x_0^4 + 900x_0^6\right),$$

$$u_{12}^{c3} = \left(4x_0^2+m^2\pi^2\right)\left(-c_{21}-3c_{22}+3c_{11}+9c_{12}\right)\left(-1+\mathrm{e}^{5x_0}\right)$$

$$b_1 = \frac{1}{8}\begin{cases} 2m_1K_{11}m_2^2 - 40K_{14}m_1^3 - 24K_{14}m_1m_2^2 - 68K_{13}m_1^2 \\ 4K_{13}m_2^2 + 41K_{12}m_1^2 - 30K_{11}m_1^3 - 4m_1^2K_{12}m_2^2 + 4K_{13} \\ 17m_1K_{11} - 2K_{12} + 32K_{14}m_1 + 32K_{13}m_1^2m_2^2 \end{cases}$$

$$b_2 = \frac{1}{8}\begin{cases} 4K_{13} - 4K_{51}m_2^2 - 4m_2^2m_1^2K_{101} + 4K_{12} - 12K_{61}m_1^3 + \\ 17K_{101}m_1^2 - 6K_{91}m_1^3 - 32K_{13}m_1^2m_2^2 - 28K_{51}m_1^2 + \\ 11K_{91}m_1 - 2m_2^2m_1K_{91} - 2K_{101} + 8K_{51}m_1^2m_2^2 + 20K_{61}m_1 \\ 12K_{61}m_1m_2^2 - 18K_{12}m_1^2 + 4K_{13}m_1^2 - 16K_{14}m_1 \\ 18m_1K_{11} + 4K_{13}m_2^2 - 24K_{14}m_1^3 + 24K_{14}m_1m_2^2 + 4K_{51} \end{cases},$$

$$b_3 = \frac{1}{8}\begin{cases} 8K_{51}m_1^2m_2^2 - 4K_{51} - 4K_{51}m_1^2 - 3K_{101}m_1^2 + 6K_{101} - \\ K_{91}m_1 + 4K_{51}m_2^2 + 4m_2^2m_1^2K_{101} - 4K_{61}m_1 - 4K_{61}m_1^3 + \\ 2K_{12} + 12K_{61}m_1m_2^2 + 2K_{91}m_1^3 - 2m_2^2m_1K_{91} - 7K_{12}m_1^2 \\ m_1K_{11} + 6K_{11}m_1^3 - 4m_1^2K_{12}m_2^2 + 2m_1K_{11}m_2^2 \end{cases}$$

$$b_4 = -b_1,$$

$$b_5 = \frac{1}{8}\begin{cases} 40K_{12}m_1^3 - 40K_{13}m_1^3 - 24K_{13}m_1m_2^2 - 4m_2^2m_1^2K_{11} + \\ 41K_{11}m_1^2 - 4K_{14} - 32K_{14}m_1^2m_2^2 - 17K_{12}m_1 + 4K_{14}m_2^2 \\ 2m_2^2m_1K_{12} - 2K_{11} + 68K_{14}m_1^2 + 32K_{13}m_1 \end{cases}$$

$$b_6 = \frac{1}{8}\begin{cases} 6K_{101}m_1^3 + 4K_{11} + 4K_{61}m_2^2 + 4K_{14} - 4K_{14}m_2^2 - 4K_{61} \\ 24K_{13}m_1m_2^2 + 32K_{14}m_1^2m_2^2 - 16K_{13}m_1 - 12K_{51}m_1^3 \\ 4m_2^2m_1^2K_{91} - 11K_{101}m_1 + 2m_2^2m_1K_{101} - 18K_{11}m_1^2 \\ 18K_{12}m_1 - 8K_{61}m_1^2m_2^2 - 24K_{13}m_1^3 - 12K_{51}m_1m_2^2 \\ 4K_{14}m_1^2 - 2K_{91} + 17K_{91}m_1^2 + 28K_{61}m_1^2 + 20K_{51}m_1 \end{cases}$$

$$b_7 = \frac{1}{8}\begin{cases} 4m_2^2m_1^2K_{11} + 2K_{101}m_1^3 - 2m_2^2m_1K_{101} + 4K_{61}m_1^2 - 2K_{11} \\ 6K_{12}m_1^3 + 8K_{61}m_1^2m_2^2 - 7K_{11}m_1^2 - 4m_2^2m_1^2K_{91} \\ 12K_{51}m_1m_2^2 - 2m_2^2m_1K_{12} + 2K_{91} - K_{12}m_1 - 4K_{51}m_1^3 \\ K_{91}m_1^2 + 4K_{61} - 4K_{61}m_2^2 - 4K_{51}m_1 + 11K_{101}m_1 \end{cases}$$

$$b_8=\begin{cases}16K_{51}c_{12}m_1^4-20K_{51}c_{12}m_1^2-32K_{61}c_{12}m_1^3+8K_{61}c_{22}m_1^3+K_4m_1\\-12K_{51}c_{11}m_1^2-4K_{61}c_{21}m_1+4K_{51}c_{21}m_1^2-2K_3m_1^2-8K_{61}c_{11}m_1^3\\+12K_{51}c_{22}m_1^2+2K_{16}m_1^2+4K_{61}c_{11}m_1+4K_{61}c_{12}m_1-4K_{61}c_{22}m_1\end{cases}$$

$$b_9=\begin{cases}4\cot(\gamma)K_{51}S_1m_1^2-6\cot(\gamma)K_{61}S_1m_1-2\cot(\gamma)K_{51}S_1\\2K_{53}m_1^2+3K_{63}m_1+K_{53}\end{cases}$$

$$b_{10}=\begin{cases}256K_{13}c_{12}m_1^4-64K_{14}c_{11}m_1^3-256K_{14}c_{12}m_1^3+64K_{14}c_{22}m_1^3\\+4K_4m_1^3-48K_{13}c_{11}m_1^2-80K_{13}c_{12}m_1^2+16K_{13}c_{21}m_1^2\\+48K_{13}c_{22}m_1^2+4K_3m_1^2+8K_{14}c_{11}m_1+8K_{14}c_{12}m_1\\-8K_{14}c_{21}m_1-8K_{14}c_{22}m_1-K_4m_1\end{cases}$$

$$b_{11}=\frac{1}{2}\begin{cases}4S_1\cot(\gamma)\left(8K_{13}m_1^2-6K_{14}m_1-K_{13}\right)+14K_{53}m_1^2\\8K_{63}m_1^3-7K_{63}m_1-K_{53}\end{cases}$$

$$b_{12}=\begin{cases}16K_{61}c_{12}m_1^4+8K_{51}c_{11}m_1^3+32K_{51}c_{12}m_1^3-8K_{51}c_{22}m_1^3\\-12K_{61}c_{11}m_1^2-4K_{51}c_{12}m_1+4K_{51}c_{21}m_1-20K_{61}c_{12}m_1^2\\+4K_{61}c_{21}m_1^2+12K_{61}c_{22}m_1^2-2K_4m_1^2-4K_{51}c_{11}m_1\\-4K_{51}c_{22}m_1-K_3m_1+K_{16}m_1\end{cases}$$

$$b_{13}=\begin{cases}2\cot(\gamma)S_1\left(2K_{61}m_1^2+3K_{51}m_1-K_{61}\right)-2K_{63}m_1^2\\3K_{53}m_1+K_{63}\end{cases}$$

$$b_{14}=\begin{cases}256K_{14}c_{12}m_1^4+64K_{13}c_{11}m_1^3+256K_{13}c_{12}m_1^3-64K_{13}c_{22}m_1^3\\-4K_3m_1^3-48K_{14}c_{11}m_1^2+8K_{13}c_{22}m_1-80K_{14}c_{12}m_1^2\\+16K_{14}c_{21}m_1^2+48K_{14}c_{22}m_1^2+4K_4m_1^2-8K_{13}c_{11}m_1\\-8K_{13}c_{12}m_1+8K_{13}c_{21}m_1+K_3m_1\end{cases}$$

$$b_{15}=\frac{1}{2}\begin{cases}4S_1\cot(\gamma)\left(8K_{14}m_1^2+6K_{13}m_1-K_{14}\right)\\+14K_{63}m_1^2-8K_{53}m_1^3+7K_{53}m_1-K_{63}\end{cases}$$

$$b_{16}=\left(1/2K_{63}m_1-1/2K_{53}-K_{53}m_1^2\right),$$

$$b_{17}=\frac{1}{4}\begin{cases}2K_{91}m_1^3+12K_{62}m_1-6m_2^2m_1K_{91}-2K_{101}\\-8K_{52}m_1^2+K_{12}m_1^2+2K_{12}+6m_1K_{11}m_2^2+4K_{52}\\-5m_1K_{11}+4m_1^2K_{12}m_2^2+2K_{101}m_2^2+7K_{101}m_1^2\\-6K_{11}m_1^3-2K_{12}m_2^2-4m_2^2m_1^2K_{101}+7K_{91}m_1\end{cases}$$

$$b_{18}=\frac{1}{4}\begin{cases}12m_1K_{11}m_2^2+28K_{52}m_1^2-14K_{62}m_1+16K_{62}m_1^3\\+23K_{12}m_1^2-2K_{52}-2K_{12}-16m_1^2K_{12}m_2^2\\2K_{12}m_2^2+13m_1K_{11}-12K_{11}m_1^3\end{cases}$$

$$b_{19}=\begin{cases}m_2^2m_1^2K_{101}+1/2K_{101}m_2^2-1/2K_{101}-4m_2^2m_1^2K_7\\-1/4K_{101}m_1^2-m_2^2m_1K_{91}-1/4K_{91}m_1-2m_2^2m_1K_8\\1/2K_7-K_7m_1^2+K_{15}+1/2K_8m_1\end{cases}$$

$$b_{20}=\frac{1}{8}\begin{cases}2K_{12}-13m_1K_{11}+16K_8m_1^3-16m_2^2m_1^2K_7+28K_7m_1^2\\12K_{11}m_1^3-2K_7+8m_1K_{11}m_2^2-23K_{12}m_1^2-14K_8m_1\\8m_2^2m_1K_8-2K_{12}m_2^2+4m_1^2K_{12}m_2^2\end{cases}$$

$$b_{21}=\frac{1}{8}\begin{cases}4K_{15}+2K_{91}m_1^3+2m_2^2m_1K_{91}-2K_{101}m_2^2\\16m_1^2K_{15}-32m_1^2K_{15}m_2^2-2K_{12}+4K_7\\10m_1K_{11}m_2^2-16m_1^2K_{12}m_2^2+6K_{11}m_1^3+2K_{12}m_2^2\\8K_7m_1^2+5m_1K_{11}+12K_8m_1+2K_{101}-7K_{101}m_1^2\\7K_{91}m_1-K_{12}m_1^2\end{cases}$$

$$b_{22}=b_{21},$$

$$b_{23}=\frac{1}{8}\begin{cases}2K_{12}-13m_1K_{11}+16K_8m_1^3-16m_2^2m_1^2K_7+28K_7m_1^2\\12K_{11}m_1^3-2K_7+8m_1K_{11}m_2^2-23K_{12}m_1^2-14K_8m_1\\8m_2^2m_1K_8-2K_{12}m_2^2+4m_1^2K_{12}m_2^2\end{cases}$$

$$b_{24}=\frac{1}{4}\begin{cases}K_{11}m_1^2+4K_{62}+2K_{91}+6m_2^2m_1K_{12}-2K_{101}m_1^3\\5K_{12}m_1-2K_{11}+4m_2^2m_1^2K_{91}-7K_{91}m_1^2+7K_{101}m_1\\12K_{52}m_1-6m_2^2m_1K_{101}-6K_{12}m_1^3-2K_{91}m_2^2\\8K_{62}m_1^2+2K_{11}m_2^2-4m_2^2m_1^2K_{11}\end{cases}$$

$$b_{25}=\frac{1}{4}\begin{cases}2K_{11}-2K_{62}-12K_{12}m_1^3+16m_2^2m_1^2K_{11}-23K_{11}m_1^2\\13K_{12}m_1-12m_2^2m_1K_{12}-2K_{11}m_2^2-16K_{52}m_1^3\\28K_{62}m_1^2+14K_{52}m_1\end{cases}$$

$$b_{26}=\frac{1}{8}\begin{cases}3K_{12}m_1-23K_{11}m_1^2+2K_{11}+4m_2^2m_1^2K_{11}-12K_{12}m_1^3\\28K_8m_1^2+2K_8-14K_7m_1-8m_2^2m_1K_{12}+16K_7m_1^3\\8m_2^2m_1K_7-2K_{11}m_2^2+16m_2^2m_1^2K_8\end{cases}$$

$$b_{27}=\frac{1}{8}\begin{cases}K_{91}-K_{11}m_1^2-2K_{11}-16K_{15}m_1+8K_8m_1^2-2K_{101}m_1^3\\2m_2^2m_1K_{101}+10m_2^2m_1K_{12}-16m_2^2m_1^2K_{11}+12K_7m_1\\2K_{11}m_2^2-2K_{91}m_2^2-6K_{12}m_1^3-7K_{91}m_1^2+7K_{101}m_1\\5K_{12}m_1-4K_8+16m_2^2m_1K_{15}\end{cases}$$

$$b_{28}=-b_{27}$$

$$b_{29}=\frac{1}{8}\begin{cases}2K_8-13K_{12}m_1-2K_{11}+14K_7m_1-8m_2^2m_1K_7\\23K_{11}m_1^2+28K_8m_1^2+8m_2^2m_1K_{12}-4m_2^2m_1^2K_{11}\\2K_{11}m_2^2-16K_7m_1^3+12K_{12}m_1^3-16m_2^2m_1^2K_8\end{cases}$$

$$b_{30}=\frac{1}{4}\begin{cases}2K_{52}+K_{101}m_1^2+K_{91}m_1-4K_{52}m_1^2+2K_{101}\\2K_{62}m_1-2K_{101}m_2^2\end{cases}$$

$$b_{31}=\frac{1}{8}\begin{cases}48m_2^2c_{31}K_{11}m_1+3K_2m_1-12K_4m_1^3-72m_2^2c_{31}K_{12}m_1^2\\+12m_2^2c_{11}K_{11}m_1+36m_2^2c_{22}K_{11}m_1+6K_4m_1-18K_3m_1^2\\+36m_2^2c_{11}K_{12}m_1^2+9K_1m_1^2+24c_{21}K_{11}m_1+324c_{12}K_{12}m_1^4\\-24c_{12}K_{11}m_1+8m_2^2c_{31}K_{12}-108c_{11}K_{12}m_1^2-180c_{12}K_{12}m_1^2\\+36c_{21}K_{12}m_1^2+4c_{21}m_2^4K_{12}+108c_{11}K_{11}m_1^3+108c_{22}K_{12}m_1^2\\-24c_{11}K_{11}m_1-8m_2^2c_{21}K_{12}-8m_2^2c_{22}K_{12}-108c_{22}K_{11}m_1^3\\+432c_{12}K_{11}m_1^3+8K_3m_1^2m_2^2-4m_2^2m_1^2K_1-4K_4m_1m_2^2\\-2K_2m_1m_2^2+36m_2^2c_{22}K_{12}m_1^2+24c_{22}K_{11}m_1-6K_2m_1^3\end{cases}$$

$$b_{32}=\frac{1}{8}\begin{cases}4S_1\cot(\gamma)\left(9K_{11}m_1+4K_{12}m_1^2-2K_{12}\right)-2m_2^2m_1K_{92}\\4m_2^2m_1^2K_{102}-12K_{63}m_1m_2^2+8K_{53}m_1^2m_2^2-4K_{53}m_2^2\\12K_{63}m_1^3+11K_{92}m_1-28K_{53}m_1^2+17K_{102}m_1^2+4K_{53}\\2K_{102}-6K_{92}m_1^3+20K_{63}m_1\end{cases}$$

$$b_{33}=\begin{cases}1/8K_2m_1-1/2K_4m_1^3+1/4K_3m_1^2-3/8K_1m_1^2\\-K_3m_1^2m_2^2+1/2m_2^2m_1^2K_1+1/2K_4m_1m_2^2-1/4K_2m_1m_2^2\\1/4K_2m_1^3-1/4K_4m_1+3/2m_2^2c_{22}K_{91}m_1-m_2^2c_{31}K_{101}m_1^2\end{cases}$$

$$b_{34}=\begin{cases}1/2S_1\cot(\gamma)K_{101}m_1^2-K_{53}m_1^2m_2^2+1/2K_{53}m_2^2\\-1/2K_{63}m_1^3-1/2K_{63}m_1+1/4K_{92}m_1^3-1/4m_2^2m_1K_{92}\\+1/2m_2^2m_1^2K_{102}+3/2K_{63}m_1m_2^2-1/8K_{92}m_1\\+3/2S_1\cot(\gamma)K_{91}m_1-3/8K_{102}m_1^2-1/2K_{53}m_1^2\\+3/4K_{102}-1/2K_{53}-S_1\cot(\gamma)K_{101}\end{cases}$$

$$b_{35}=\begin{cases}8c_{13}m_1^4+2c_{13}m_1^2+2c_{24}m_1^2-2c_{11}K_4m_1-8c_{11}K_4m_1^3\\ +4c_{21}K_3m_1^2+2c_{22}K_4m_1+16c_{12}K_3m_1^4+8c_{22}K_4m_1^3\\ +4c_{12}K_3m_1^2+1/2c_{24}+c_{21}K_3\end{cases}$$

$$b_{36}=\begin{cases}16K_{53}c_{12}m_1^4+4S_1\cot(\gamma)K_3m_1^2-8K_{63}c_{11}m_1^3-32K_{63}c_{12}m_1^3\\ +8K_{63}c_{22}m_1^3-2S_1\cot(\gamma)K_4m_1-12K_{53}c_{11}m_1^2-20K_{53}c_{12}m_1^2\\ +4K_{53}c_{21}m_1^2+12K_{53}c_{22}m_1^2+4K_{63}c_{11}m_1+4K_{63}c_{12}m_1\\ +4K_{63}c_{21}m_1-4K_{63}c_{22}m_1\end{cases}$$

$$b_{37}=\begin{cases}6\cot(\gamma)K_{63}S_1m_1-2\cot(\gamma)K_{53}S_1+4\cot(\gamma)K_{53}S_1m_1^2\\ 1/2K_pS_1^2+2K_pS_1^2m_1^2\end{cases}$$

$$b_{38}=\begin{cases}16K_4c_{12}m_1^4+8K_3c_{11}m_1^3-8K_3c_{22}m_1^3+4K_4c_{12}m_1^2\\ +4K_4c_{21}m_1^2+4c_{14}m_1^3-4c_{23}m_1^3\\ +2K_3c_{11}m_1-2K_3c_{22}m_1+K_4c_{21}+c_{14}m_1-c_{23}m_1\end{cases}$$

$$b_{39}=\begin{cases}16K_{63}c_{12}m_1^4+4\cot(\gamma)K_4S_1m_1^2+8K_{53}c_{11}m_1^3+32K_{53}c_{12}m_1^3\\ -8K_{53}c_{22}m_1^3+2\cot(\gamma)K_3S_1m_1-12K_{63}c_{11}m_1^2-20K_{63}c_{12}m_1^2\\ +4K_{63}c_{21}m_1^2+12K_{63}c_{22}m_1^2-4K_{53}c_{11}m_1-4K_{53}c_{12}m_1\\ +4K_{53}c_{21}m_1+4K_{53}c_{22}m_1\end{cases}$$

$$b_{40}=\left(4\cot\gamma K_{63}S_1m_1^2+6\cot\gamma K_{53}S_1m_1+2K_pS_1^2m_1-2\cot\gamma K_{63}S_1\right),$$

$$b_{41}=\begin{cases}K_{52}m_1^2m_2^2+5/2K_{62}m_1+1/4K_7m_2^2-3/2K_{62}m_1^3\\ -2m_2^2m_1^2K_7-5/4K_8m_1+3/4K_8m_1^3-7/2K_{52}m_1^2\\ -1/4K_7+7/4K_7m_1^2-1/2K_{52}m_2^2+1/2K_{52}\\ 7/4m_2^2m_1K_8-3/2K_{62}m_1m_2^2\end{cases}$$

$$b_{42}=\begin{cases}1/2K_{62}m_1+1/4K_8m_1^3-1/2K_{52}m_1^2+1/4K_7m_1^2+\\ 3/2K_{62}m_1m_2^2+1/2K_{52}m_2^2-1/2K_{15}+1/4K_7-\\ 1/2K_{52}-1/4K_7m_2^2-1/2K_{62}m_1^3-K_{52}m_1^2m_2^2+1/4K_8m_1\\ 1/2m_1^2K_{15}+1/2K_{15}m_2^2+1/4m_2^2m_1K_8-m_1^2K_{15}m_2^2\end{cases}$$

$$b_{43}=\begin{cases}3/4K_8m_1^3-7/4K_7m_1^2+1/4K_7+5/4K_8m_1\\ 3/4m_2^2m_1K_8-1/4K_7m_2^2\end{cases}$$

$$b_{44}=\begin{cases}1/4K_8m_1-1/2m_1^2K_{15}+1/2K_{15}+1/4K_7m_2^2\\ -1/2K_{15}m_2^2-1/4K_8m_1^3+m_1^2K_{15}m_2^2+3/4m_2^2m_1K_8\\ 1/4K_7m_1^2-1/4K_7-2m_2^2m_1^2K_7\end{cases}$$

$$b_{45}=\begin{cases}2m_2^2m_1^2K_8+\frac{7}{4}m_2^2m_1K_7+\frac{5}{2}K_{52}m_1+1/2K_{62}m_2^2-\frac{7}{4}K_8m_1^2\\ -K_{62}m_1^2m_2^2-\frac{1}{2}K_{62}+\frac{1}{4}K_8-\frac{5}{4}K_7m_1-\frac{1}{4}K_8m_2^2\\ -\frac{3}{2}K_{52}m_1m_2^2+\frac{7}{2}K_{62}m_1^2-\frac{3}{2}K_{52}m_1^3+\frac{3}{4}K_7m_1^3\end{cases}$$

$$b_{46}=\begin{cases}\frac{1}{2}K_{62}-\frac{1}{4}K_8+\frac{1}{4}m_2^2m_1K_7+\frac{1}{4}K_7m_1^3+2m_2^2m_1K_{15}+\frac{1}{4}K_7m_1\\ +\frac{1}{4}K_8m_2^2-K_{15}m_1+\frac{3}{2}K_{52}m_1m_2^2+\frac{1}{2}K_{62}m_1^2-\frac{1}{2}K_{62}m_2^2\\ -\frac{1}{4}K_8m_1^2+K_{62}m_1^2m_2^2-\frac{1}{2}K_{52}m_1-\frac{1}{2}K_{52}m_1^3\end{cases}$$

$$b_{47}=\begin{cases}5/4K_7m_1+1/4K_8m_2^2-1/4K_8-3/4m_2^2m_1K_7\\ 3/4K_7m_1^3+7/4K_8m_1^2\end{cases}$$

$$b_{48}=\begin{cases}\frac{1}{4}K_8m_1^2-\frac{1}{4}K_7m_1^3+K_{15}m_1-\frac{1}{4}K_7m_1+\frac{3}{4}m_2^2m_1K_7\\ +\frac{1}{4}K_8-\frac{1}{4}K_8m_2^2+2m_2^2m_1^2K_8\end{cases}$$

$$b_{49}=\left(16K_{15}c_{21}m_2^4-m_2^2m_1^2K_1-8K_{15}c_{21}m_2^2-8K_{15}c_{22}m_2^2+8K_{15}c_{31}m_2^2\right),$$

$$b_{50}=\begin{cases}m_2^2m_1^2K_{102}-1/2K_{102}-1/4K_{102}m_1^2+1/2K_{102}m_2^2\\ m_2^2m_1K_{92}-1/4K_{92}m_1-2S_1\cot(\gamma)K_{15}\end{cases}$$

$$b_{51}=\begin{cases}1/2K_2m_1-1/2K_2m_1^3-1/2K_2m_1m_2^2+K_1m_1^2-8c_{11}K_{62}m_1^3\\ -32c_{12}K_{62}m_1^3+8c_{22}K_{62}m_1^3-m_2^2m_1^2K_1-12c_{11}K_{52}m_1^2\\ -4c_{21}K_{62}m_1+4c_{11}K_{62}m_1+4c_{12}K_{62}m_1-4c_{22}K_{62}m_1\\ +12c_{22}K_{52}m_1^2-20c_{12}K_{52}m_1^2+4c_{21}K_{52}m_1^2+16c_{12}K_{52}m_1^4\end{cases}$$

$$b_{52}=\begin{cases}1/2K_{92}m_1^3+1/2K_{102}m_2^2+7/4K_{92}m_1+4S_1\cot(\gamma)K_{52}m_1^2\\ +7/4K_{102}m_1^2-1/2K_{102}-m_2^2m_1^2K_{102}-3/2m_2^2m_1K_{92}\\ 6S_1\cot(\gamma)K_{62}m_1-2S_1\cot(\gamma)K_{52}\end{cases}$$

$$b_{53}=\begin{cases}4m_2^2c_{11}K_8m_1+16m_2^2c_{31}K_8m_1-\frac{1}{4}K_2m_1-\frac{1}{2}K_1m_1^2+8c_{12}K_7m_1^4\\ -4m_2^2c_{21}K_7-6c_{11}K_7m_1^2-10c_{12}K_7m_1^2+\frac{1}{4}K_2m_1m_2^2+\frac{1}{4}K_2m_1^3\\ +8m_2^2c_{22}K_7m_1^2-12m_2^2c_{22}K_8m_1+8m_2^2c_{11}K_7m_1^2-16m_2^2c_{31}K_7m_1^2\\ +2c_{11}K_8m_1+2c_{21}K_7m_1^2-4c_{11}K_8m_1^3-16c_{12}K_8m_1^3+2c_{12}K_8m_1\\ +4c_{22}K_8m_1^3-2c_{21}K_8m_1+6c_{22}K_7m_1^2-2c_{22}K_8m_1+4m_2^2c_{31}K_7\\ -4m_2^2c_{22}K_7+8c_{21}m_2^4K_7\end{cases}$$

$$b_{54}=\begin{cases}2S_1\cot(\gamma)K_7m_1^2-1/4K_{102}m_2^2-S_1\cot(\gamma)K_7-3S_1\cot(\gamma)K_8m_1\\ +1/4K_{92}m_1^3+1/4K_{102}+1/4m_2^2m_1K_{92}-\frac{7}{8}K_{102}m_1^2-\frac{7}{8}K_{92}m_1\end{cases}$$

$$b_{55}=\begin{cases}1/2K_1m_1-1/2K_1m_1^3-K_2m_1^2+16c_{12}K_{62}m_1^4+8c_{11}K_{52}m_1^3\\ +4c_{21}K_{62}m_1^2+4c_{21}K_{52}m_1-4c_{11}K_{52}m_1-4c_{12}K_{52}m_1\\ +4c_{22}K_{52}m_1-12c_{11}K_{62}m_1^2+12c_{22}K_{62}m_1^2+m_2^2m_1^2K_2\\ 32c_{12}K_{52}m_1^3-8c_{22}K_{52}m_1^3-1/2K_1m_1m_2^2-20c_{12}K_{62}m_1^2\end{cases}$$

$$b_{56}=\begin{cases}4S_1\cot(\gamma)K_{62}m_1^2+6S_1\cot(\gamma)K_{52}m_1-1/2K_{92}m_2^2\\ +7/4K_{102}m_1-1/2K_{102}m_1^3-7/4K_{92}m_1^2+m_2^2m_1^2K_{92}\\ -3/2m_2^2m_1K_{102}-2S_1\cot(\gamma)K_{62}+1/2K_{92}\end{cases}$$

$$b_{57}=\begin{cases}4c_{22}K_7m_1^3+6c_{11}K_8m_1^2+2c_{12}K_7m_1-2c_{22}K_7m_1-2c_{21}K_7m_1\\ +2c_{11}K_7m_1+4m_2^2c_{22}K_8-4m_2^2c_{31}K_8-6c_{22}K_8m_1^2-2c_{21}K_8m_1^2\\ -4c_{11}K_7m_1^3+4m_2^2c_{21}K_8-8c_{12}K_8m_1^4-16c_{12}K_7m_1^3\\ -8c_{21}m_2^4K_8+10c_{12}K_8m_1^2+\frac{1}{4}K_1m_1-\frac{1}{4}K_1m_1^3-\frac{1}{2}K_2m_1^2\\ \frac{1}{4}K_1m_1m_2^2+16m_2^2c_{31}K_7m_1-8m_2^2c_{11}K_8m_1^2-12m_2^2c_{22}K_7m_1\\ 4m_2^2c_{11}K_7m_1+16m_2^2c_{31}K_8m_1^2-8m_2^2c_{22}K_8m_1^2\end{cases}$$

$$b_{58}=\frac{1}{8}\begin{cases}7K_{102}m_1-2K_{102}m_1^3-7K_{92}m_1^2-2m_2^2m_1K_{102}-16S_1\cot\gamma K_8m_1^2\\ 2K_{92}-24S_1\cot(\gamma)K_7m_1+8S_1\cot(\gamma)K_8-2K_{92}m_2^2\end{cases}$$

$$b_{59}=\left(1/4K_{102}m_1^2-1/2K_{102}m_2^2+1/4K_{92}m_1+1/2K_{102}\right),$$

$$b_{60}=\begin{Bmatrix}-1/2c_{11}K_2m_1+1/2c_{21}K_1m_1^2-1/2c_{14}m_1^2m_2^2-1/2c_{23}m_1^2m_2^2\\+1/2c_{12}K_1m_1^2-1/2c_{13}m_1^2-1/2c_{24}-1/2c_{22}K_2m_1^3\\-1/2c_{22}K_2m_1-1/2m_2^2c_{11}K_2m_1-m_2^2c_{21}K_1+1/2c_{12}K_1m_1^4\\+1/2m_2^2c_{22}K_2m_1+1/2m_2^2c_{22}K_1m_1^2-m_2^2c_{31}K_1m_1^2\\+1/2c_{21}m_2^4K_1+1/2m_2^2c_{11}K_1m_1^2-c_{32}m_1^2m_2^2-1/2c_{24}m_2^4\\+1/2c_{11}K_2m_1^3+1/2c_{21}K_1-1/2c_{13}m_1^4+c_{24}m_2^2-1/2c_{24}m_1^2\end{Bmatrix}$$

$$b_{61}=\begin{Bmatrix}m_2^2c_{31}K_{102}+c_{22}K_{92}m_1-c_{11}K_{92}m_1-c_{12}K_{92}m_1-1/2c_{22}K_{92}m_1^3\\+c_{21}K_{92}m_1-3/2c_{11}K_{102}m_1^2-5/2c_{12}K_{102}m_1^2-m_2^2c_{21}K_{102}\\+1/2c_{21}K_{102}m_1^2-m_2^2c_{22}K_{102}+2c_{12}K_{92}m_1^3+3/2c_{22}K_{102}m_1^2\\+1/2c_{12}K_{102}m_1^4+1/2c_{21}m_2^4K_{102}+1/2m_2^2c_{22}K_{102}m_1^2\\-2m_2^2c_{31}K_{92}m_1+1/2m_2^2c_{11}K_{92}m_1+1/2m_2^2c_{11}K_{102}m_1^2\\-1/2S_1\cot(\gamma)K_1m_1^2-m_2^2c_{31}K_{102}m_1^2+1/2S_1\cot(\gamma)K_2m_1\\+3/2m_2^2c_{22}K_{92}m_1+1/2c_{11}K_{92}m_1^3\end{Bmatrix}$$

$$b_{62}=\frac{1}{2}\begin{Bmatrix}2S_1\cot(\gamma)K_{102}-K_pS_1^2m_1^2-K_pS_1^2m_2^2+K_pS_1^2\\+S_1\cot(\gamma)K_{102}m_1^2+3S_1\cot(\gamma)K_{92}m_1\end{Bmatrix}$$

$$b_{63}=\begin{Bmatrix}-1/2m_2^2c_{22}K_1m_1-1/2c_{14}m_1m_2^2-m_2^2c_{31}K_2m_1^2\\+1/2m_2^2c_{22}K_2m_1^2-1/2c_{11}K_1m_1+1/2m_2^2c_{11}K_1m_1\\+1/2c_{22}K_1m_1+1/2m_2^2c_{11}K_2m_1^2+1/2c_{22}K_1m_1^3\\+1/2c_{12}K_2m_1^4+1/2c_{21}m_2^4K_2+1/2c_{21}K_2m_1^2-m_2^2c_{21}K_2\\+1/2c_{23}m_1m_2^2+1/2c_{12}K_2m_1^2+1/2c_{14}m_1^3-1/2c_{23}m_1^3\\+1/2c_{14}m_1-1/2c_{23}m_1+1/2c_{21}K_2-1/2c_{11}K_1m_1^3\end{Bmatrix}$$

$$b_{64}=\begin{Bmatrix}m_2^2c_{31}K_{92}m_1^2+1/2m_2^2c_{11}K_{92}m_1^2-1/2S_1\cot(\gamma)K_1m_1\\-3/2m_2^2c_{22}K_{102}m_1+m_2^2c_{31}K_{92}+c_{12}K_{102}m_1-c_{22}K_{102}m_1\\+1/2S_1\cot(\gamma)K_2m_1^2-1/2m_2^2c_{11}K_{102}m_1+2m_2^2c_{31}K_{102}m_1\\+c_{11}K_{102}m_1-2c_{12}K_{102}m_1^3-m_2^2c_{21}K_{92}-3/2c_{11}K_{92}m_1^2\\+3/2c_{22}K_{92}m_1^2+1/2c_{21}K_{92}m_1^2+1/2c_{22}K_{102}m_1^3\\-c_{21}K_{102}m_1-1/2c_{11}K_{102}m_1^3-5/2c_{12}K_{92}m_1^2-m_2^2c_{22}K_{92}\\+1/2c_{12}K_{92}m_1^4+1/2c_{21}m_2^4K_{92}+1/2m_2^2c_{22}K_{92}m_1^2\end{Bmatrix}$$

$$b_{65}=\begin{Bmatrix}K_pS_1^2m_1-S_1\cot(\gamma)K_{92}+1/2S_1\cot(\gamma)K_{92}m_1^2\\+3/2S_1\cot(\gamma)K_{102}m_1\end{Bmatrix}$$